

REC'D JUN 17 1963

PB 181476

Price \$1.50

MTRB LIBRARY

**CRACK PROPAGATION IN LOW-CYCLE  
FATIGUE OF MILD STEEL**

**SSC-143**

BY

**S. T. ROLFE AND W. H. MUNSE**

**SHIP STRUCTURE COMMITTEE**

For sale by the U. S. Department of Commerce, Office of Technical Services,  
Washington 25, D. C.

# SHIP STRUCTURE COMMITTEE

## MEMBER AGENCIES:

BUREAU OF SHIPS, DEPT. OF NAVY  
MILITARY SEA TRANSPORTATION SERVICE, DEPT. OF NAVY  
UNITED STATES COAST GUARD, TREASURY DEPT.  
MARITIME ADMINISTRATION, DEPT. OF COMMERCE  
AMERICAN BUREAU OF SHIPPING

## ADDRESS CORRESPONDENCE TO:

SECRETARY  
SHIP STRUCTURE COMMITTEE  
U. S. COAST GUARD HEADQUARTERS  
WASHINGTON 25, D. C.

1 May 1963

Dear Sir:

Structural experience both with ships and other structures has indicated that fatigue-type failures, particularly low-cycle fatigue, are an important structural problem. In order to evaluate the influence of a few load cycles at high-stress levels upon the mechanical properties of ship steels, a project on "Low-Cycle Fatigue" was initiated at the University of Illinois. Herewith is a copy of the second progress report, SSC-143, Crack Propagation in Low-Cycle Fatigue of Mild Steel by S. T. Rolfe and W. H. Munse.

This project is being conducted under the advisory guidance of the Committee on Ship Structural Design of the National Academy of Sciences-National Research Council.

Comments concerning this report are solicited.

Yours sincerely,



T. J. Fabik  
Rear Admiral, U.S. Coast Guard  
Chairman, Ship Structure  
Committee

Serial No. SSC-143  
Second Progress Report  
of  
Project SR-149  
to the  
SHIP STRUCTURE COMMITTEE

on  
CRACK PROPAGATION IN LOW-CYCLE FATIGUE  
OF MILD STEEL

by  
S. T. Rolfe and W. H. Munse  
University of Illinois  
Urbana, Illinois

under  
Department of the Navy  
Bureau of Ships Contract NObs-77008  
BuShips Index No. NS-731-034

transmitted through  
Committee on Ship Structural Design  
Division of Engineering and Industrial Research  
National Academy of Sciences-National Research Council

under  
Department of the Navy  
Bureau of Ships Contract NObs-84321  
Index No. S-R 009 03 01, Task 2004

Washington, D. C.  
U.S. Department of Commerce, Office of Technical Services  
1 May 1963

## ABSTRACT

The investigation reported is concerned with crack propagation in low-cycle fatigue of mild-steel plate specimens and has indicated that during crack propagation the type of loading cycle will affect markedly the fatigue behavior.

Several types of reversed loading cycles have been included in the investigation, namely constant load, reduced loads and constant stress. In the constant-load tests the stress increases throughout the test as the crack propagates, and the rate of crack propagation continuously increases. If the load range is reduced throughout a test (reduced-load test) so as to produce constant net-section stresses, the rate of crack growth will decrease throughout the test. In the constant-stress tests the stress range was maintained constant during the test. In this latter use, the rate of fatigue crack propagation remained constant after a short initial period.

Constant-stress tests were conducted at stress levels ranging from  $\pm 27$  ksi to  $\pm 36$  ksi, on 3/4-in. thick specimens with widths of 5 in. and 7 in., at test temperatures of 78 F and -40 F and for both unaged and aged specimens.

It was found that the fatigue crack propagation behavior during a constant-stress test may be divided into an initial, linear, and final stage. A hypothesis relating the rate of crack growth and the stress has been developed to describe the behavior during the various stages of propagation.

# CONTENTS

	<u>Page</u>
Introduction. . . . .	1
Fatigue Crack Propagation Review . . . . .	2
Object and Scope . . . . .	5
Nomenclature . . . . .	5
Description of Experimental Investigation . . . . .	5
Description of Specimens . . . . .	5
Test Equipment . . . . .	7
Test Procedure . . . . .	7
Measurements During Tests . . . . .	10
Crack Length . . . . .	10
Strain Gage Measurements . . . . .	10
Photoelastic Strain Measurements . . . . .	12
Discussion and Analysis of Tests . . . . .	13
Effect of Type of Loading on Fatigue Behavior . . . . .	13
Constant-Load Tests . . . . .	13
Reduced-Load Tests . . . . .	14
Constant-Stress Tests . . . . .	16
Significance of Type of Loading . . . . .	17
Rate of Fatigue Crack Propagation . . . . .	18
Effect of Temperature and Aging . . . . .	32
Summary and Conclusions . . . . .	34
Summary . . . . .	34
Conclusions . . . . .	35
References . . . . .	37
Appendix A	
Study of Compressive Load Carried by Partially Cracked Specimen . . . . .	41
Appendix B	
Correlation of Existing Theories with Initial Stage of Crack Propagation . . . . .	45
Appendix C:	
Strain Distributions . . . . .	48

NATIONAL ACADEMY OF SCIENCES-NATIONAL RESEARCH COUNCIL  
Division of Engineering & Industrial Research

SR-149 PROJECT ADVISORY COMMITTEE

"Low-Cycle Fatigue"

for the

COMMITTEE ON SHIP STRUCTURAL DESIGN

Chairman:

J. M. Frankland  
Consultant, Mechanics Division  
National Bureau of Standards

Members:

J. A. Bennett  
Chief, Mechanical Metallurgy  
National Bureau of Standards

B. J. Lazan  
Head, Department of Aeronautical and  
Mechanical Engineering  
University of Minnesota

J. D. Lubahn  
Director, Materials Research Laboratory  
Colorado School of Mines

Dana Young  
Technical Vice President  
Southwest Research Institute

Liaison:

John Vasta  
Bureau of Ships, Dept. of the Navy

## INTRODUCTION

### Low-Cycle Fatigue

The major objective in many fatigue investigations has been to determine the fatigue limits and corresponding S-N curves for members constructed of various materials for very long service life. Recently, however, there has been an increase in interest in the fatigue behavior of structures at high stress levels and low numbers of cycles of loading, usually referred to as low-cycle fatigue. Although no clear distinction exists between low-cycle and long-life fatigue, the upper limit of low-cycle fatigue is usually considered to be  $10^4$  to  $10^5$  cycles.

To better study fatigue behavior, and particularly low-cycle fatigue, it is desirable to divide the total fatigue life of a member into an initiation stage and a propagation stage. This is done because fatigue-crack initiation is more likely to be influenced by the conditions near the point of origin while fatigue-crack propagation is more likely to be affected by the conditions throughout the entire cross section that the crack traverses.<sup>1</sup> Various theories which attempt to explain the mechanism of fatigue-crack initiation have been developed. Since the investigation reported herein was concerned primarily with fatigue-crack propagation, theories of fatigue initiation are not discussed in this report but may be found in many other references.<sup>2-9</sup> As may be noted in the literature, the division between initiation and propagation usually depends upon the type of observation used in the investigation, i.e., phenomenological or microscopic. In this and most other studies of fatigue-crack propagation, a phenomenological observation, the occurrence of a visual surface crack, has been employed to establish the beginning of the propagation stage.

The study of fatigue-crack propagation is important since it is the propagation of a crack which ultimately leads to failure of a member by fatigue. It has been suggested that in certain types of structures, a fatigue crack may grow to some "critical" length and then lead to a sudden catastrophic brittle fracture.<sup>10</sup> For other structures a knowledge of the rate of crack growth may be important in establishing inspection procedures to protect against failure.

These and other factors make a knowledge of the process of fatigue-crack propagation an important part of our understanding of fatigue.

#### FATIGUE CRACK PROPAGATION REVIEW

In 1936, De Forest<sup>11</sup> noted that fatigue results were usually somewhat ambiguous because there was no distinction between the number of cycles required to initiate fatigue cracks and the number of cycles required to propagate the cracks to failure. He stated that in addition to determining the maximum stress level at which a fatigue crack would not propagate, it was also necessary to determine the rate at which a given crack would propagate. He conducted rotating-beam tests of low-carbon steel specimens and found the rate of crack propagation to increase markedly with the applied stress level. In addition, he found that the stress level and number of cycles of load required to initiate a crack were largely determined by the surface condition of the specimen while the resistance to crack growth was independent of the initial surface.

Wilson<sup>12</sup> tested 12-in.-wide steel plates with a 2-7/8-in. central saw cut as a stress-raiser and found that the rate of crack propagation remained constant for fatigue cracks of lengths up to 0.6-in. Strain aging was found to decrease the rate of crack propagation but changing the test temperature within the range of 120 F to -40 F appeared to have no effect on the rate of crack growth. It should be noted, however, that a relatively low-stress level was used ( $\pm 16$  ksi) and that the rates were determined for fairly short fatigue-crack lengths (0.6-in.).

Head<sup>13, 14</sup> considered the fatigue mechanism to consist of a cycle-dependent work-hardening which occurs at the tip of a crack. He postulated that, when the region ahead of the crack has work-hardened to the true fracture strength of the material, the crack propagates through this region and the process is repeated. Then, for any given set of conditions he concluded that the rate of crack growth is a function of the crack length ( $dl/dN = kl^{3/2}$ ).

McClintock<sup>15</sup> conducted theoretical and experimental studies of crack growth in bars subjected to fully plastic cycles of torsion. The strain distri-



bution was computed theoretically for this type of specimen using a sand-hill analogy. The material was assumed to be fully plastic, nonwork-hardening and to have a negligible Bauschinger effect. Experimental results were in good agreement with the theoretical predictions.

Hult<sup>16</sup> derived an expression for the redistribution of stress and strain in front of a growing crack in a twisted bar. The results of this analysis were used in connection with a simple fracture criterion, based on the maximum shear strain, to determine the initial rate of growth of a fatigue crack.

Fatigue tests of thin plate specimens of 24S-T3 aluminum alloy were conducted by Martin and Sinclair.<sup>17</sup> They suggest that the fatigue mechanism may be considered to consist of three parts, namely, (a) crack nucleation or initiation, (b) crack propagation by fatigue, and (c) crack propagation by creep. They conclude that it is not possible to describe crack growth in terms of the theoretical stress at the tip of the crack since the crack length affects the rate of growth.

Liu<sup>18</sup> conducted constant load tests on 4-in. wide 2024-T3 aluminum alloy sheet specimens and developed an expression for rate of crack growth for a semi-infinite sheet in terms of the crack length and a stress dependent propagation factor,  $C$ . His expression,  $dl/dN = Cl$ , gave consistent results for the major portion of the life of the specimens. However, the expression was valid only for crack lengths which varied from about 0.07-in. to about 0.16-in. As the crack grew beyond a length of 0.16-in. it was necessary to modify the expression to predict the total fatigue life of the specimens because of the change in nominal stress.

Frost and Dugdale<sup>19, 20</sup> concluded from theoretical considerations that the strain distribution around a small internal slit in wide plates remains geometrically similar as the slit grows. This conclusion was verified using the results of fatigue tests on mild steel plates. It was found that the rate of crack propagation was proportional to crack length, i.e.,  $dl/dN = kl$ . However, this relationship was valid for only crack lengths less than 1/8 the width of the plate.

A method for determining the rate of fatigue-crack propagation in sheet specimens of 2024-T3 and 7075-T6 aluminum alloys has been developed by

McEvily and Illg.<sup>21-23</sup> Semi-empirical expressions using  $K_n \sigma$  (theoretical stress-concentration factor modified for size effect times the stress based on the remaining cross-sectional area) were developed and verified experimentally for stress ratios of  $R = 0$  and  $R = -1$ . The effective stress concentration factor,  $K_n$ , is Neuber's<sup>24</sup> stress concentration factor modified for the effect of finite plate width as determined by Howland.<sup>25</sup> Sheet specimens with a central stress raiser were tested and values of  $d\ell/dN$  vs.  $K_n \sigma$  were used to determine the empirical relationship:

$$\log d\ell/dN = C_1 K_n \sigma - C_2 - C_3 \frac{\sigma_{end}}{K_n \sigma - \sigma_{end}}$$

where  $d\ell/dN$  = rate of crack growth

$C_1, C_2,$  and  $C_3$  = constants

$K_n$  = effective stress concentration factor

$\sigma$  = stress based on the remaining or instantaneous cross sectional area

$\sigma_{end}$  = fatigue limit (or stress at  $10^8$  cycles).

Weibull<sup>26-29</sup> tested aluminum sheets under conditions of constant tensile stress based on the remaining area and found that the rate of crack growth was independent of the crack length after an initial transition period. A relationship between stress amplitude and growth rate was developed and may be expressed in the following form:

$$\frac{d\ell}{dN} = k (\sigma - \sigma_0)^n$$

where  $k$  and  $n$  = constants

$\sigma_0$  = lower limit of the applied stress below which a crack did not propagate.

Massonnet and his associates<sup>30</sup> studied the rate of propagation under conditions of constant load and also constant stress based on the remaining area for specimens subjected to repeated bending. They concluded that the general relationship developed by Weibull for axial load on aluminum specimens was valid also for mild steel specimens subjected to bending.

## Object and Scope

The purpose of the investigation reported herein was to study the parameters affecting fatigue crack propagation at high stress levels and to develop a basic expression for fatigue crack growth. Flat plates were tested to study the manner in which various parameters such as type of loading cycle, temperature, geometry, and aging affect the rate of fatigue-crack growth. In addition, the results of the tests were correlated with existing theories of fatigue crack growth.

## Nomenclature

$\ell$  = crack length measured from center-line of specimen (initial crack length plus fatigue crack), in.

$\ell_0$  = initial crack length, radius of initial central hole plus saw cut, in.

N = number of cycles of loading

$d\ell/dN$  = rate of fatigue crack propagation, in./cycle

a = constant

K = crack growth parameter

W = width of plate specimen, in.

$N_L$  = number of cycles of loading required to propagate a fatigue crack a given distance L.

$\sigma$  = stress = applied load divided by the remaining or instantaneous net cross-sectional area.

"Average" maximum strain (Measured) = strain just ahead of the crack tip measured with strain gages.

## DESCRIPTION OF EXPERIMENTAL INVESTIGATION

### Description of Specimens

The specimens used to study crack propagation were 3/4-in.-thick by 4-ft-long flat plates with either a 5-in. or 7-in. width and initial central notches of various lengths, as may be seen in Fig. 1. These notches served to reduce the time of crack initiation, to minimize the effect of prior stress history on crack propagation, and to predetermine the position of the fatigue crack for ease of crack-growth measurement.

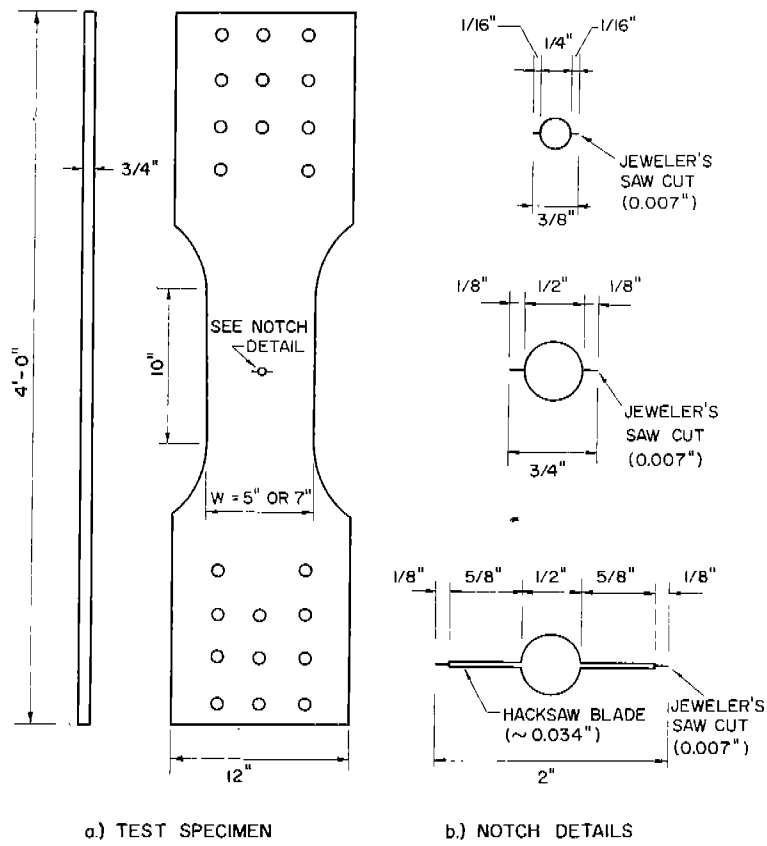


FIG. 1. SPECIMEN AND NOTCH DETAILS

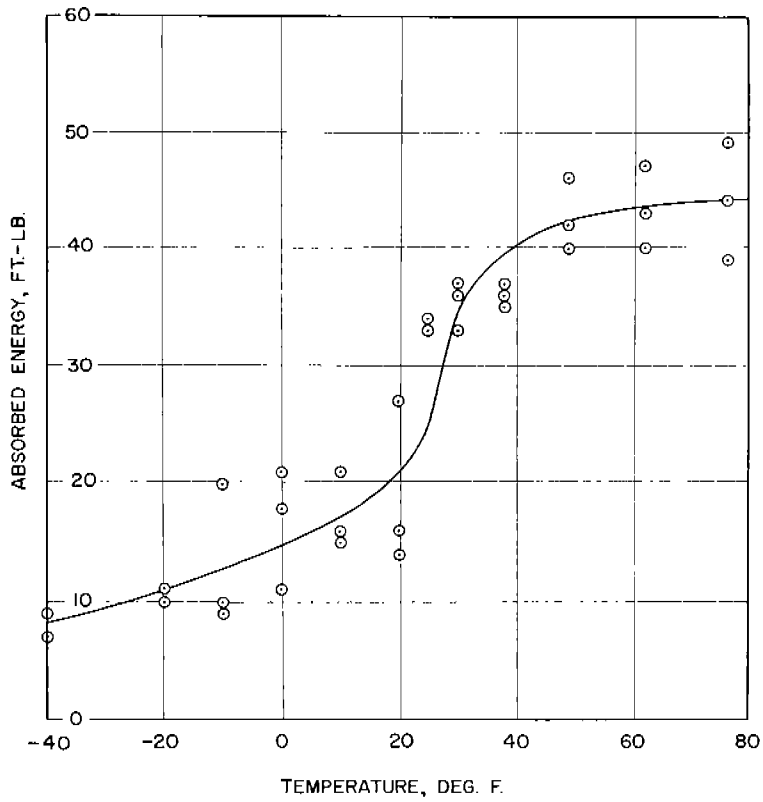


FIG. 2. RESULTS OF CHARPY V-NOTCH IMPACT TESTS

All of the fatigue cracks initiated from a .007-in.-wide jeweler's saw cut which was used to produce a sharp initiating notch. The two widths investigated (5-in. and 7-in.) were chosen to study propagation over as great a distance as possible and still be within the load capacity of the available fatigue testing machines. The specimens were polished in the longitudinal direction to facilitate the observations and measurements of cracks. Although this surface treatment may affect slightly the initiation of the fatigue cracks, it would have little or no effect on the crack propagation.<sup>1, 11</sup>

The material used in these tests was an ABS-C as-rolled ship steel. The lower yield point of the material was 39.4 ksi and the ultimate strength was 70.6 ksi. These properties are typical of mild steel and are presented in Table 1 along with the other mechanical properties of the material. The 15-ft-lb Charpy V-notch temperature was about 0°F as may be seen in Fig. 2. The axial fatigue limit for polished plain plate specimens was approximately  $\pm 27$  ksi.

#### Test Equipment

All fatigue tests were conducted in the 200,000-lb capacity University of Illinois lever-type fatigue testing machines. A detailed description of the operation of the machines may be found elsewhere.<sup>31</sup>

Throughout the investigation the alignment of the machines was carefully controlled and the bending strains were found to be less than 10 per cent of the axial strains. These strains corresponded to an eccentricity of less than .03-in. Considering the size of the specimens and testing machines, this was considered to be a relatively small amount of bending. As pointed out later in the discussion, this slight eccentricity of the load had little effect on the test results.

#### Test Procedure

Three types of repeated load cycles were studied in this investigation, namely, constant load, reduced load, and constant stress. Two types were basically complete reversal of load with the mean load equal to zero and one was essentially complete reversal of stress.

In the constant-load tests the tensile and compressive loads were kept

TABLE 1  
SUMMARY OF MATERIAL PROPERTIES

(A) Tensile Test Data (Standard ASTM 0.505-in. Diameter)\*

Temperature deg. F	Lower Yield Stress (ksi)	Upper Yield Stress (ksi)	Ultimate Strength (ksi)	Elongation in 2-in. %	Reduction of Area %	Fracture Stress (ksi)
78	39.4	41.6	70.6	35.2	60.0	133.8
-40	43.5	46.1	76.0	35.0	60.0	146.6
<u>Aged Specimens (90 min. at +150° C)</u>						
78	40.1	43.3	70.6	33.5	61.6	140.2
-40	44.6	47.9	80.9	34.5	62.4	162.7

\*(All specimens parallel to direction of rolling each value average of two tests.)

(B) Chemical (Check) Analysis - Percent

C	Mn	P	S	Si	Cu	Cr	Ni	Al
0.24	0.69	0.022	0.030	0.20	0.22	0.08	0.15	0.034

constant throughout the entire test.

In the reduced-load tests, both the tensile and compressive loads were decreased periodically throughout the test to maintain a constant stress on the remaining cross-sectional area during the test.

In the constant stress tests the maximum tensile stress was based on the remaining cross-sectional area while the maximum compressive stress was based on the original net cross-sectional area. Therefore the maximum tensile load was decreased periodically throughout the test but the maximum compressive load was maintained.

The procedure for conducting the constant stress tests was as follows. Initially the maximum tensile and compressive stresses were based on the original net area (gross area minus the area of the initial hole and sawed notch). As the fatigue crack propagated, the surface crack length was measured, the remaining uncracked area was determined, and the tensile load was changed to maintain a constant tensile stress on the remaining area. The frequency with which the crack length was measured and the load adjusted was such that the maximum change or adjustment in tensile stress was never greater than 2.0 ksi.

During the compressive load cycle, the fatigue crack closes fully and the cracked portion of the specimen continues to carry load. Verification of the fact that the cracked portion does carry compressive load is presented in Appendix A. Therefore the maximum compressive load (and thus the maximum compressive stress) was kept constant throughout the entire test.

All tests were conducted at room temperature (approximately 78 F) except for four constant-stress low-temperature tests which were conducted at -40 F. To cool the latter specimens, four special containers were placed adjacent to the central notched region of the plates and dry ice was placed in the containers in direct contact with the specimens. Thermocouples mounted on the plate surface were used to record the surface temperatures in the vicinity of the notch. Although the temperature of the specimen at the cooling containers was lower than -40 F, the temperature of the test section was maintained between -40 F and -50 F by controlling the amount of dry ice in the containers. This slight temperature variation was due to the cooling method used and was

not considered great enough to affect the results of the crack-propagation studies.

## MEASUREMENTS DURING TESTS

### Crack Length

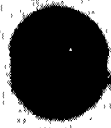
In all tests, the total crack length (initial drilled hole and saw cut plus the fatigue crack) was measured from the centerline of the specimens. This measurement was made on both surfaces and an average of the four measurements was designated as the crack length ( $l$ ) at any given number of cycles of loading ( $N$ ). During the tests a 10X microscope and a dye-penetrant were used to determine the location of the tip of the crack. Using this procedure it was possible to measure the surface crack lengths to the nearest .005-in.

In several tests radiographs were made at various surface crack lengths to determine whether the surface crack measurements gave an accurate indication of the remaining area. The results of the radiographic examinations indicated that the fatigue cracks propagated with essentially a full-thickness front. This fact is evident in the series of radiographs presented in Fig. 3 for a constant-load test. Figure 3a shows the initial drilled hole and saw cuts. The remaining radiographs then show the fatigue cracks propagating from the notches. The apparent fanning-out of the crack in Fig. 3e indicates that as the crack propagates the angle which the crack makes with the direction of loading changes. However, even near the end of a test the interior crack front was not advancing ahead of the surface crack. Therefore, the surface crack length measurements do in fact give an accurate representation of the cracked area.

### Strain Gage Measurements

Foil strain gages were mounted ahead of the expected fatigue crack location on the plate surface of several specimens. Periodically during the fatigue tests, as the fatigue cracks propagated, the machine was stopped to manually load the specimen to different stress levels and to determine the strains. By repeating this procedure at various crack lengths it was possible to obtain the longitudinal strain gradient ahead of the crack at various stages of the test. A photograph showing a typical strain gage layout is presented in Fig. 4b.





a)  $N = 0$



b)  $N = 1476$



c)  $N = 2880$

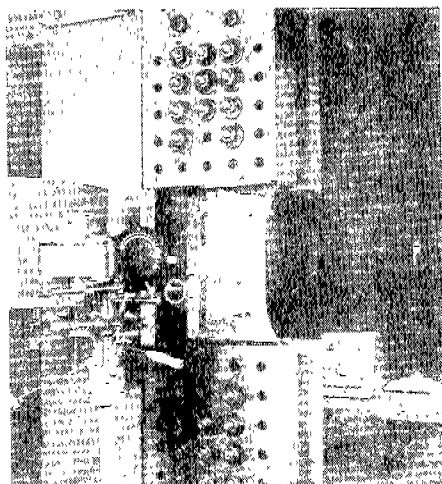


d)  $N = 3553$

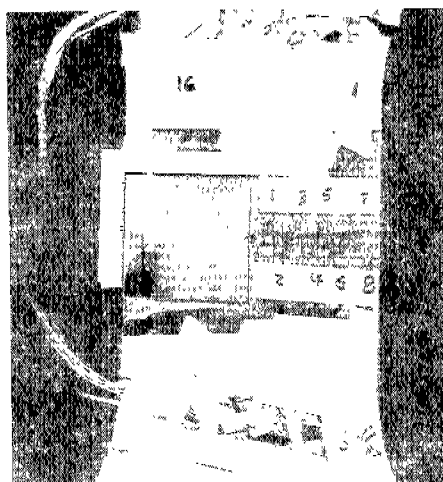


e)  $N = 3899$

FIG. 3. RADIOGRAPHS OF CRACK GROWTH IN CONSTANT-LOAD TEST



a) SPECIMEN AND EQUIPMENT USED TO MEASURE SURFACE STRAIN DISTRIBUTION



b) TRANSPARENT PLASTIC AND GAGES FOR STRAIN DISTRIBUTION STUDIES

FIG. 4. TYPICAL SPECIMEN AND EQUIPMENT FOR STRAIN DISTRIBUTION STUDIES

#### Photoelastic Strain Measurements

A photoelastic stress analysis technique was used to determine the over-all strain distribution ahead of the fatigue crack at various crack lengths or at various stages of the test. As the load is applied, the surface strains in the specimen are transmitted to a plastic sheet bonded to the surface of the specimen. Using a reflection polariscope, contours for various values of principal strain difference ( $\epsilon_1 - \epsilon_2$ ) can be seen directly in the transparent plastic sheet. These contours (isochromatics) were photographed for later reproduction and analysis. Figure 4a is a photograph showing a specimen in the fatigue testing machine, the photoelastic test equipment and the camera used to record the strain distribution at various crack lengths. Figure 4b is a close-up of the transparent plastic sheet with a fatigue crack that has propagated about 1.4-in. A more detailed discussion of this photoelastic strain measuring technique may be found elsewhere.<sup>32</sup>

## DISCUSSION AND ANALYSIS OF TESTS

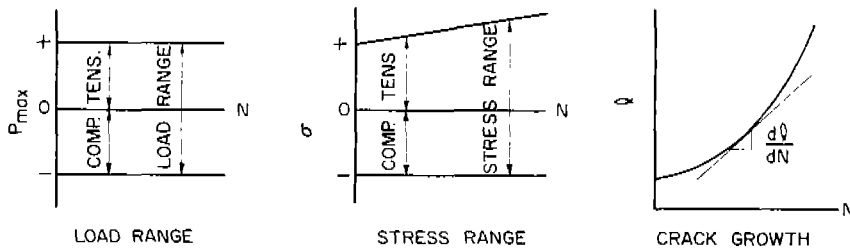
### Effect of Type of Loading on Fatigue Behavior

Prior to crack initiation, the stress distribution in a specimen is usually well defined on the basis of the initial geometry. Once a crack initiates, however, the stress at the point of initiation and the stress distribution ahead of the crack both change. Additional changes in the stress distribution ahead of the crack tip occur during propagation and, at failure, the stress condition is quite different than it was prior to initiation. Since fatigue crack propagation will be affected by the stress distribution during the test, the type of repeated loading used is very important in any study of crack propagation. This is especially true when results of small-scale laboratory test specimens are used to predict the behavior of actual structures.

### Constant-Load Tests

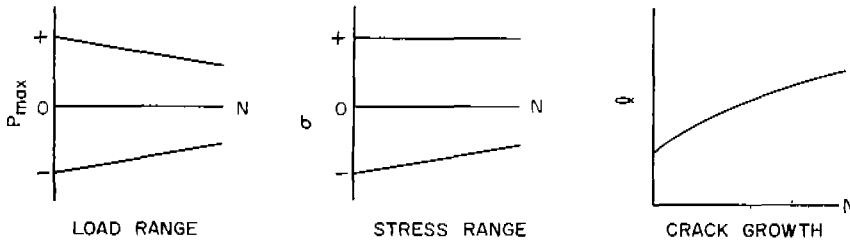
In a constant-load fatigue test, the load is kept constant as the fatigue crack grows thereby causing the maximum tensile stress to increase during the test. However, since the fatigue crack closes during the compressive cycle, the maximum compressive stress remains essentially constant throughout the test. Thus, because the load range is kept constant, the maximum stress range continuously increases throughout the test. As a consequence, the rate of crack growth ( $dl/dN$ ) increases also. This general behavior is shown schematically in Fig. 5a.

In the constant-load tests the fatigue cracks initially propagated in a direction perpendicular to the direction of applied loading. When, as a result of the increase in crack length, the maximum tensile stress reached the yield strength of the material, the mode of failure began to change. At that time the surface of the crack at mid-thickness remained perpendicular to the applied load but near the surface of the member, the crack gradually changed direction and shear lips developed. These shear lips continued to grow until the entire fracture surface was oriented in a plane or planes making an angle of  $45^\circ$  with the direction of applied load. After the cracks had reached this latter stage, complete failure occurred within a very few additional cycles of loading. A

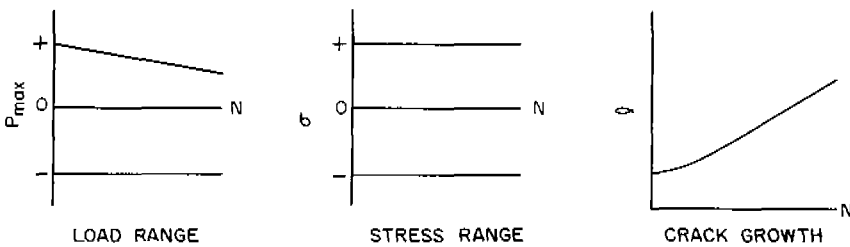


a) CONSTANT LOAD TEST

FIG. 5. TYPES OF REPEATED LOADING



b) REDUCED LOAD TEST

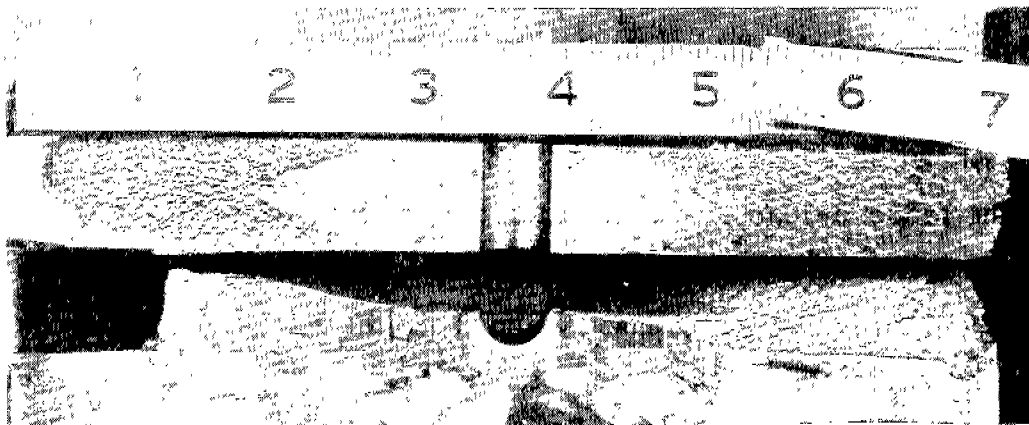


c) CONSTANT STRESS TEST

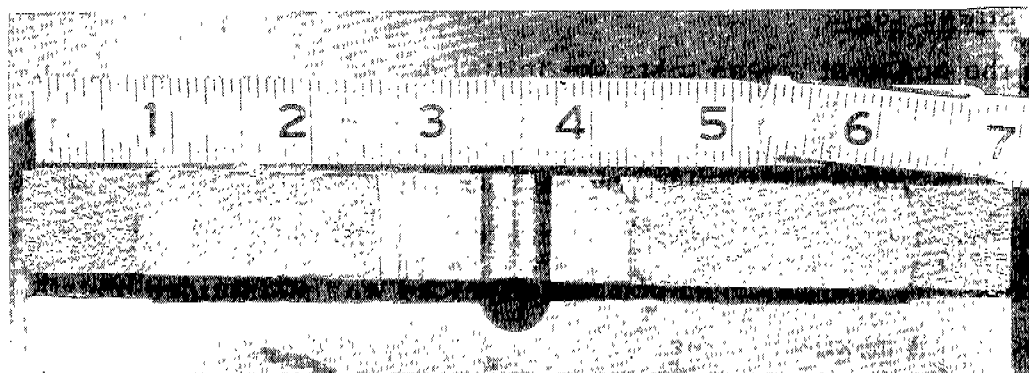
photograph of this type of fatigue crack propagation is presented in Fig. 6a. As may be seen in the photograph, when the crack was about 7/8-in. long (measured from the center line) the mode of failure began to change. At this point, the maximum tensile stress was 39.2 ksi, whereas the yield strength of this material is 39.4 ksi. Thus the mode of fracture at any given location appears to be a function of the maximum stress on the member.

Reduced-Load Tests

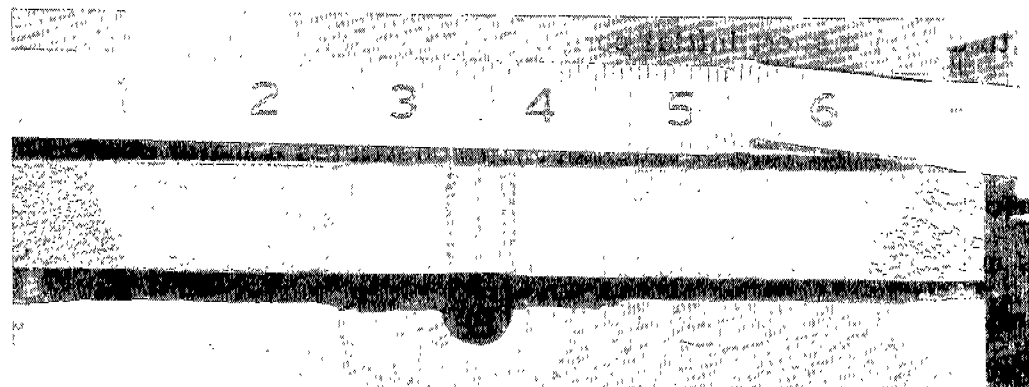
In these tests the initial maximum tensile and compressive stresses were based on the original net area. As the fatigue crack propagated, both the tensile and compressive loads were similarly decreased so that the maximum stresses, based on the remaining uncracked area, were maintained constant. Thus the maximum tensile stress remains constant but, since the cracked portion continues



a) CONSTANT LOAD TEST



b) REDUCED LOAD TEST



c) CONSTANT STRESS TEST

FIG. 6. TYPICAL FRACTURE SURFACES

to carry compressive load, the maximum compressive stress and the maximum stress range decrease throughout the test. As a result of the decrease in stress range, the rate of fatigue crack growth decreases also. This general type of behavior is shown in Fig. 5b.

In the reduced-load tests, the direction of the fatigue cracks remained perpendicular to the direction of the applied load throughout the tests, as may be seen in Fig. 6b. Note the symmetry and the relatively blunt full-thickness front of the fatigue crack. In this case the test was continued until the crack was less than an inch away from the edges, at which time the specimen was loaded statically to failure.

#### Constant-Stress Tests

In the constant stress tests the initial maximum tensile and compressive stresses were based on the original net area, just as in the previous two types of tests. To maintain the maximum tensile stress constant, the tensile load was decreased periodically throughout the test. Since the cracked portion carried compression, the maximum compressive load was maintained constant. Thus, a constant maximum stress range was obtained by decreasing the tensile load but keeping the compressive load constant. This general behavior may be seen schematically in Fig. 5c.

In this type of test the rate of crack growth increased with increasing crack length during a short initial period of the test and then remained essentially constant. A study of this initial increase in rate of growth and the extensive period of linear rate of crack growth constitutes a major portion of this investigation.

As may be seen in Fig. 6c, the fatigue crack for this type of loading was essentially the same as that observed in the reduced-load tests, and consequently, the surface crack measurements give a good indication of the cracked area even though a slight eccentricity in propagation can be observed. After the crack had propagated across the major portion of the specimen the fatigue test was stopped and the specimen was loaded statically to failure.

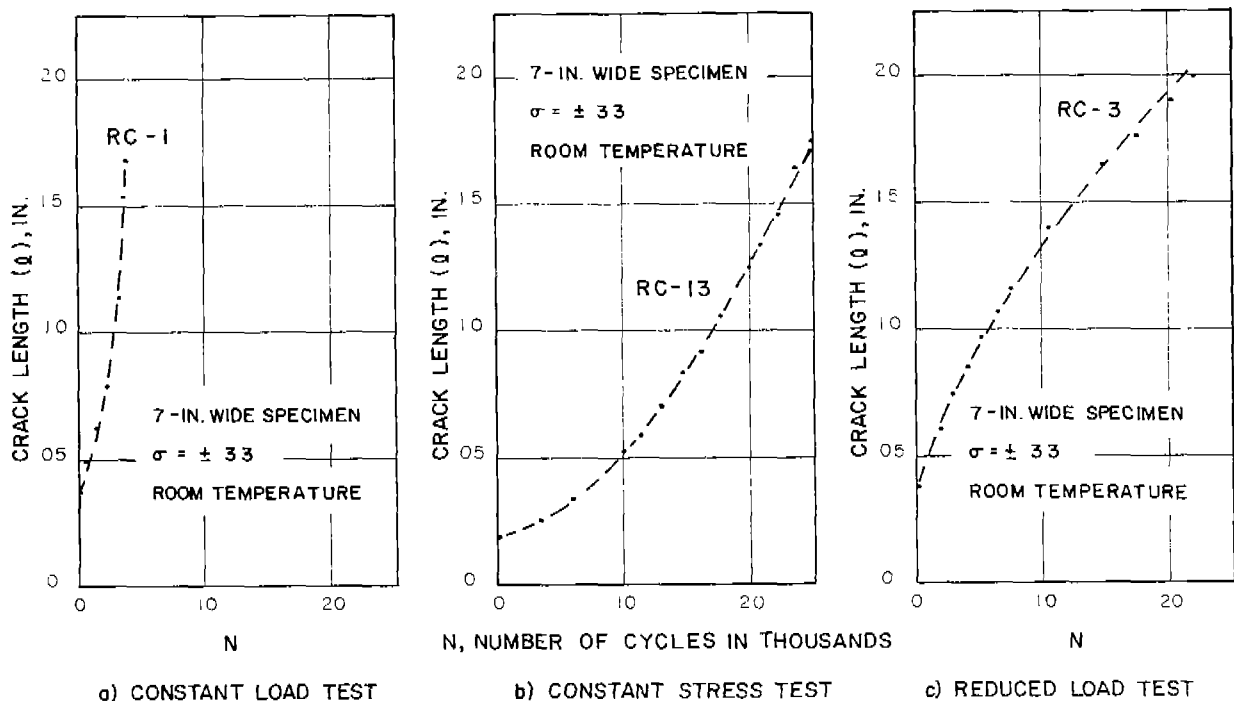


FIG. 7. FATIGUE CRACK PROPAGATION FOR THREE TYPES OF REPEATED LOADING

The crack growth curves for the three types of specimens shown in Fig. 6 are presented in Fig. 7 and indicate the actual behavior as portrayed by the crack propagation data.

Significance of Type of Loading

One of the principal purposes of laboratory fatigue studies is to obtain information to predict the behavior of actual structures. Most of these investigations are conducted on fairly small specimens in which the stress distribution ahead of a crack changes markedly as the crack propagates (constant-load tests). However, in a structure, depending upon its size, a fatigue crack can generally grow for some distance without significantly changing the over-all stress distribution in the structure. To approximate this condition in the laboratory specimens, the studies of the constant-load tests must be limited to only very small crack lengths (usually less than 1/8 the plate width). However, a closer approximation to the behavior of actual structures may be obtained with constant-stress tests, since in these tests the over-all stress distribution ahead of the crack is not markedly affected by the increase in crack length. Thus it would

appear that constant-stress tests more closely approximate the fatigue crack propagation behavior of actual structures than do the other types of tests.

An important point that the different types of loading cycles bear out is the significant effect that the tensile and compressive loadings have on the propagation rate. This is demonstrated schematically in Fig. 5 where the crack-growth curve is changed when the stress and loading are varied. The greatest rate of crack propagation is obtained under the constant-load condition. If the tensile load is decreased to provide the constant-stress condition, a reduced propagation rate is obtained and, finally, if the compressive load is also decreased to provide the reduced load condition, a further reduction in crack growth is obtained.

#### Rate of Fatigue Crack Propagation

Stages of Crack Growth: The study of various loading cycles suggested that for constant-stress tests, the rate of fatigue crack growth ( $d\ell/dN$ ) might be proportional to the applied stress for the major portion of the life of a specimen. Therefore it has been assumed that,

$$d\ell/dN = K \sigma \quad (1)$$

where  $d\ell/dN$  and  $\sigma$  are defined as before and  $K$  is a coefficient that depends on material, geometry and test temperature.

To verify this hypothesis, constant-stress tests were conducted at stress levels ranging from  $\pm 27$  ksi to  $\pm 36$  ksi, on 3/4-in. thick specimens with widths of 5-in. and 7-in., at test temperatures of 78 F and -40 F and for both unaged and aged specimens. A summary of the test conditions for all constant-stress tests is presented in Table 2.

For all tests, crack-length measurements were made and curves of crack length  $\ell$  vs. number of cycles of loading  $N$  were obtained. These general relationships between  $\ell$  and  $N$  may be separated into an initial, linear, and final stage as shown schematically in Fig. 8.

The initial stage is a relatively short period in the total life of the specimen and is affected by the stress level, the number of cycles to crack initiation, initial geometry and increasing stress field around the crack tip. However, this is the period for which most expressions for fatigue crack growth have been de-



TABLE 2  
SUMMARY OF CONSTANT-STRESS TEST RESULTS

Specimen Number	Stress (ksi)	Width* (in.)	Test Temperature deg. F	Initial Rate of Crack Propagation**	Linear Rate of Crack Propagation***
(A) <u>Unaged</u>					
RC-32	$\pm 36$	5	78	205	600
RC-33	$\pm 33$	5	78	83	230
RC-16	$\pm 30$	7	78	28	95
RC-31	$\pm 30$	5	78	32	77
RC-21	$\pm 27$	7	78	13	40
RC-30	$\pm 27$	5	78	12	29
RC-20	$\pm 30$	7	-40	12	25
RC-27	$\pm 30$	5	-40	8	21
RC-7	0 to +33	7	78	11	15
(B) <u>Aged</u> (90 min. at 150 C)					
RC-35	$\pm 33$	5	78	85	237
RC-19	$\pm 30(\pm 27)$	7	78	19	54 (30)
RC-34	$\pm 30$	5	78	27	50
RC-18	$\pm 27(\pm 30)$	7	78	9	25 (60)
RC-29	$\pm 27$	5	78	13	16
RC-26	$\pm 30$	7	-40	10	25
RC-28	$\pm 30$	5	-40	12	20

\*Total initial central crack length,  $2 l_0 = \frac{3}{8}$  in.

\*\*Measured at  $l = 0.20$ -in. (in./cycle  $\times 10^6$ )

\*\*\*Refers to linear stage of crack growth (in./cycle  $\times 10^6$ )

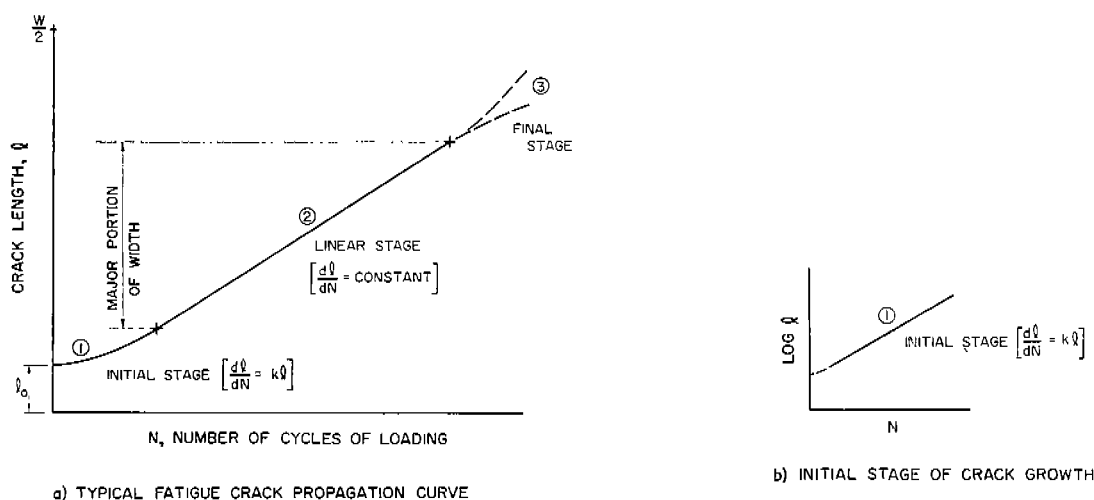


FIG. 8. STAGES OF CRACK GROWTH FOR CONSTANT-STRESS TESTS

veloped. During this period it is generally found that the rate of crack growth is proportional to the crack length and may be expressed as,

$$dl/dN = k l \quad (2)$$

where  $k$  is a constant.

Much of the previous work on fatigue crack propagation in plates has been based on the assumption of constant stress in a semi-infinite plate. After the crack has grown a small amount, this assumption is no longer valid for finite plate widths. Consequently, Eq. 2 is valid only for relatively short crack lengths.

In this investigation it has been found that the rate of crack growth increases with increasing crack length during the initial stage of crack propagation, and that a constant relationship exists between  $\log l$  and  $N$ , as is shown in Fig. 8b. Thus, the results of this investigation agree with the results of other investigations for very short crack lengths (see Appendix B).

After the initial stage, a linear rate of crack growth was observed during the major portion of the life for all specimens, i.e.,

$$\frac{dl}{dN} = \text{Constant.} \quad (3)$$

As the crack neared the edges of the specimens, eccentricity in the specimens and edge effects began to affect the growth markedly. This latter

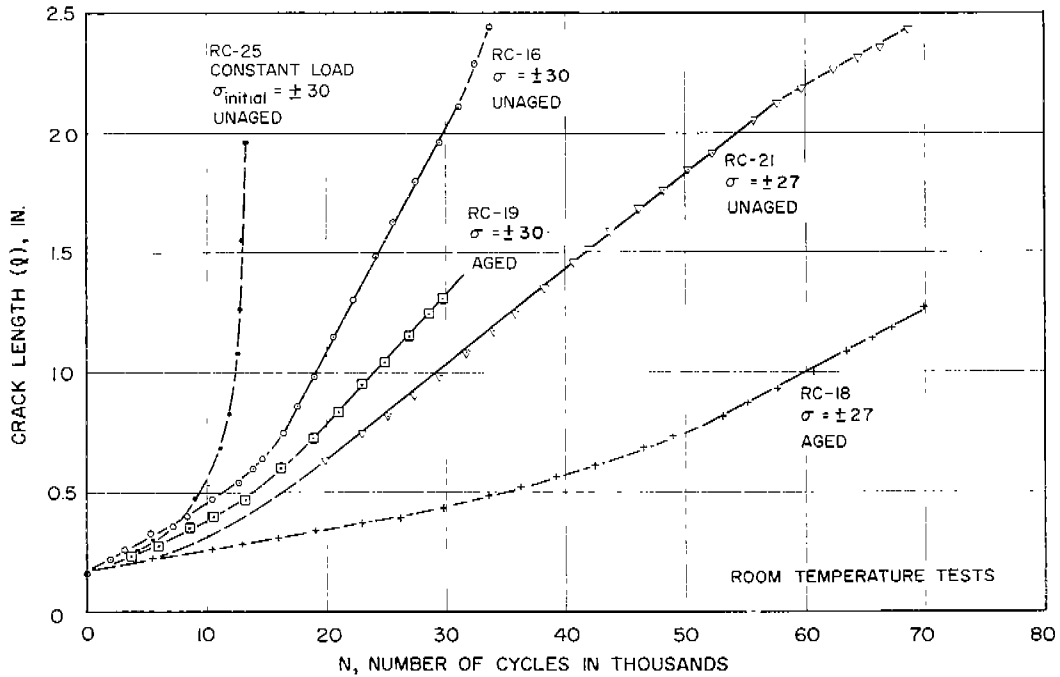


FIG. 9. FATIGUE CRACK PROPAGATION FOR 7-IN.-WIDE SPECIMENS

stage has been called the final stage. Once the linear rate of crack growth had been determined over a sufficiently long crack length in any particular test, the test was usually stopped.

Analysis of Linear Stage of Crack Growth: The major portion of this investigation consisted of an analysis of the relationship between the rates of fatigue crack growth in the linear stage and such parameters as stress level, temperature, aging and geometry.

Curves of  $l$  vs.  $N$  for all tests are presented in Figs. 9-11. From these figures, rates of crack propagation were determined by measuring the slope of the curves at  $l = 0.20$ -in. (just after crack initiation) and after a constant rate of propagation had been reached. The linear rates of crack propagation and the rates at  $l = 0.20$ -in. for all tests are presented in Table 2.

The linear stage crack growth data of Figs. 9, 10, and 11 have been analyzed in terms of Eq. 1. For tests of specimens having the same width, test temperature and aging, a definite linear relationship exists between  $\log (dl/dN)$  and  $\log \sigma$  as shown in Fig. 12. The general equation of this relationship is:

$$\log \frac{dl}{dN} = \log K + a \log \sigma \quad (4)$$

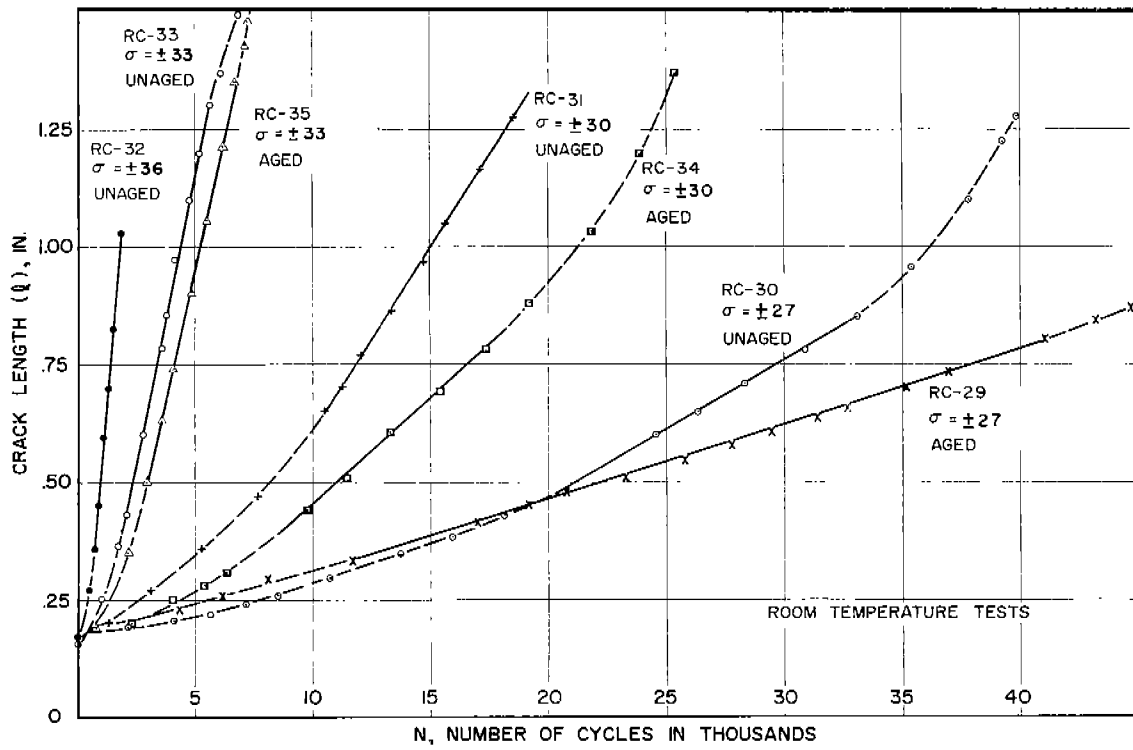


FIG. 10. FATIGUE CRACK PROPAGATION FOR 5-IN.-WIDE SPECIMENS

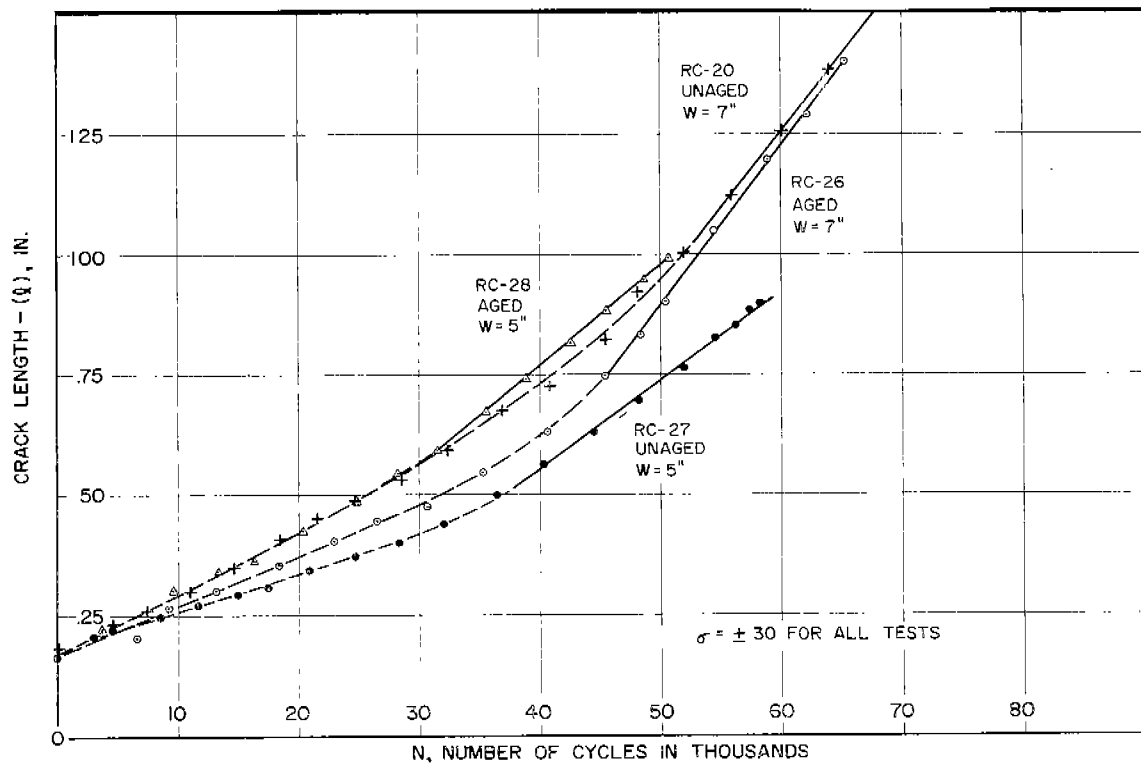


FIG. 11. FATIGUE CRACK PROPAGATION AT -40 DEG. F.

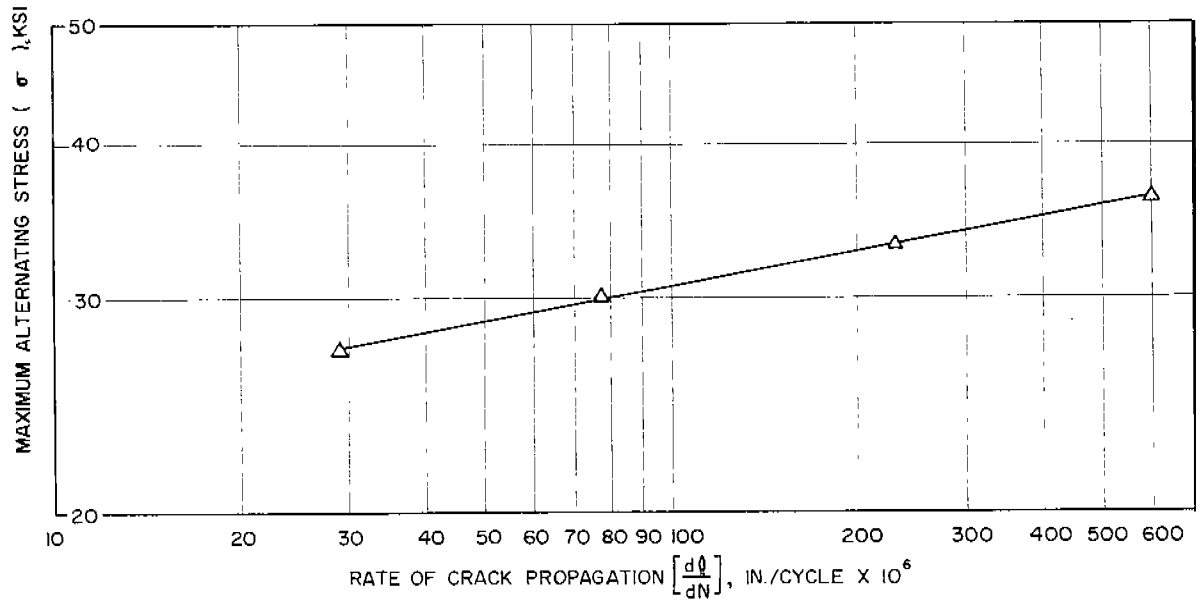


FIG. 12. RATE OF CRACK GROWTH VS. STRESS

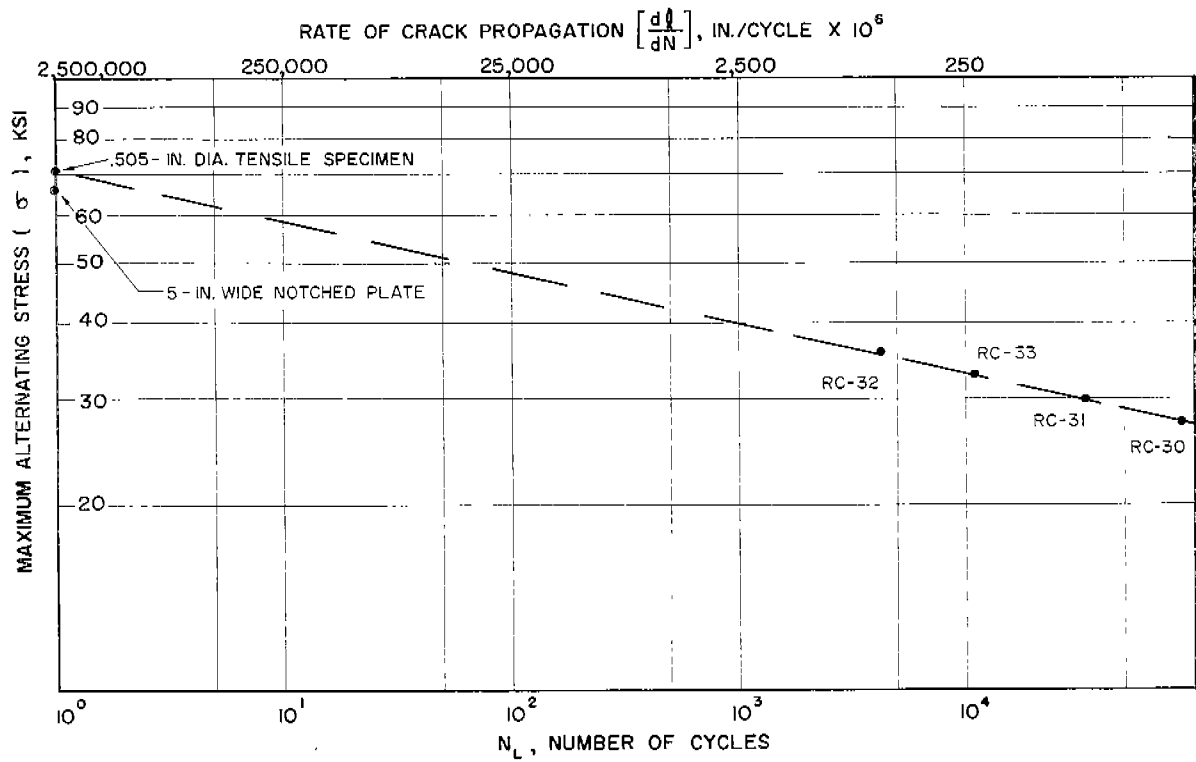


FIG. 13. STRESS VS. PROPAGATION LIFE

or

$$\frac{d\ell}{dN} = K \sigma^a \tag{5}$$

which is of the same form as Eq. 1.

Thus, the experimental results verify the general hypothesis that, after the initial stage of crack growth, the rate of fatigue crack propagation is primarily a function of the stress on the remaining area.

Using the fact that the rate of crack propagation is primarily a function of the stress, one can determine the number of cycles of loading required to propagate a crack through any distance L at a given stress level,  $\sigma$ . Thus, for a given stress and the corresponding constant rate of crack propagation, the following expression can be used to determine the relationship between stress and propagation life.

$$N_L = \frac{L}{d\ell/dN} \tag{6}$$

where

$N_L$  = number of cycles required to propagate a crack a given distance, L.

The linear stage values of crack growth and stress for the 5-in.-wide specimens tested at the same temperature and with no prior artificial aging were as follows:

<u>Stress</u> <u>ksi</u>	<u>Rate of</u> <u>Crack Growth</u> <u>in/cycle x 10<sup>6</sup></u>
± 36	600
± 33	230
± 30	77
± 27	29

Using these values and Eq. 6, the total propagation lives then may be computed (neglecting the effect of the initial stage of crack propagation) and the relationship between stress and propagation life determined as shown in Fig. 13. If the relationship is extended to  $N = 1$  (one application of failure load or in other words a static tensile test) a close approximation to the tensile coupon strength (70.6 ksi) or the strength of a 5-in.-wide centrally notched plate loaded to failure

(65.5 ksi) is obtained. The equation of this relationship is:

$$N^m \sigma = C \quad (7)$$

This is of the general form used by Tavernelli and Coffin<sup>33</sup> to predict low-cycle fatigue behavior,

$$N^{\frac{1}{2}} \Delta \epsilon_t = \frac{q_f}{2} \quad (8)$$

where

$\Delta \epsilon_t$  = plastic tensile strain range

$q_f$  = true fracture strain measured in tensile test

It should be noted that Eqs. 7 and 8 are similar and are both related to conditions in a tensile test. However, much more work remains to be done on crack to better define the fatigue crack propagation life in the very low-cycle fatigue range.

Evaluation of Crack Growth Parameters: For a given material, thickness, stress level, temperature, etc., the coefficients  $\underline{K}$  and  $\underline{a}$  in Eq. 5 are functions of geometry only. During a test the geometry changes (crack length increases) and therefore it would be expected that  $\underline{K}$  and/or  $\underline{a}$  should change also. This change in  $\underline{K}$  and/or  $\underline{a}$  would be apparent in the rate of crack growth and in the strain distribution around the crack front.

A change in the rate of crack growth does occur during the initial stage and may be seen in the crack propagation curves in Figs. 9-11. This is evident further from a comparison of the initial (at  $l = 0.20$ -in.) and linear values of  $dl/dN$  presented in Table 2. A plot of the initial  $dl/dN$  (at  $l = 0.20$ -in.) vs.  $\sigma$  and the linear  $dl/dN$  vs.  $\sigma$  is presented in Fig. 14, where it can be seen that the slope of both curves,  $\underline{a}$ , is the same but that  $\underline{K}$ , the propagation intercept of the lines, increases as the crack length increases. The value of  $\underline{K}$  increases with increasing crack length only up to the beginning of the linear stage of crack growth. Thus,  $\underline{a}$  appears to be a constant for this material and  $\underline{K}$  a factor related to crack length during the initial stage of crack propagation and a constant during the linear stage.

For a given material, if  $\underline{K}$  increases with crack length, the extent and

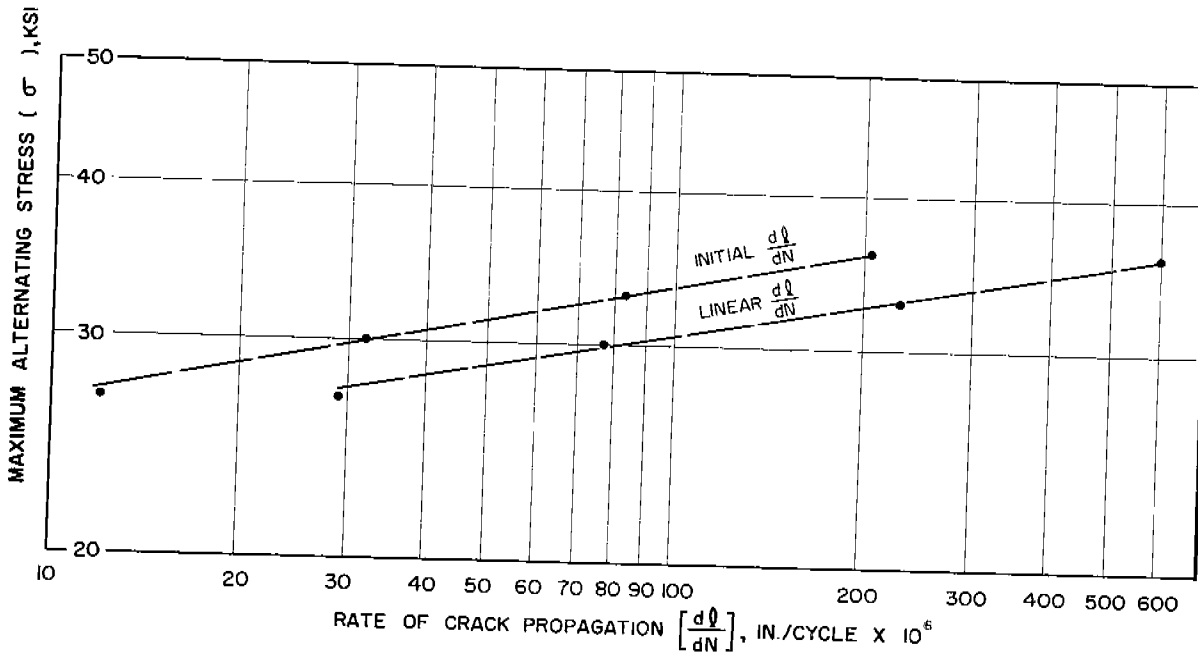


FIG. 14. INITIAL AND LINEAR RATES OF CRACK GROWTH VS. STRESS

magnitude of the strain field ahead of the propagating crack would also increase. Frost<sup>19, 20</sup> and Liu<sup>18</sup> noted this behavior as a growth of the "plastic zone" ahead of the crack.

For an elliptical crack in a plate Timoshenko<sup>34</sup> expresses the elastic stress as being related to  $(1 + 2 d/b)$  where  $d$  and  $b$  are the major and minor axes of the ellipse. If a fatigue crack can be approximated by an elliptical slit of large  $d/b$  ratio, then for a constant value of  $b$ , the stress would increase with increasing crack length (increasing major axis  $d$ ).

Evaluation of Strain Distribution: Strain gages were used to determine the effect of crack length on the strain distribution ahead of a propagating fatigue crack. It was not possible to obtain the value of strain at the tip of the crack because of the finite size of a strain gage. However, by using small gage lengths (1/4 in. and 1/16 in.) the effect of crack length on the "average" maximum strain (measured) near the crack tip could be determined. In some cases, the strain gages were placed slightly above or below the expected crack path so that strain measurements could be obtained after the crack has propagated beyond a gage.

The 0-to-tension increments of strain were examined to study the effect



of crack length on the strain near the tip of the crack. As the crack propagated toward a gage, hysteresis loops were obtained in the strain records. In addition, when the load was removed at any time during a test, some permanent strain was recorded. This permanent strain was used as the "zero" reference to determine the incremental tensile strain for that particular crack length. The incremental strain distributions for 0-to-tension loadings at various crack lengths are presented in Appendix C.

Initially the measured maximum tensile strain near the saw cut is some multiple of the computed average strain across the net section. Then, as the fatigue crack initiates and the crack length increases, the measured maximum tensile strain near the crack tip appears to increase further. This increase in strain with crack length, even though the load is decreased to maintain a constant stress, occurs until the rate of crack growth reaches the linear stage. After reaching the linear stage the maximum strain near the tip of the crack appears to remain essentially constant.

The average increase in the maximum strain, i.e., the ratio of measured maximum strain near the tip of the crack during the linear rate of crack growth to the measured maximum strain for a crack length of only 0.20-in. (just after crack initiation) was 2.90. Similarly, the average increase in rate of crack growth for these same tests (ratio of linear rate of growth to rate of growth at  $l = 0.20$ -in.) was 2.63. Thus it appears that during the initial stage as well as the linear stage of propagation the rate of crack growth is approximately proportional to the maximum strain near the crack tip.

To investigate the effect of initial crack length on the initial stress distribution and initial rate of crack growth, fatigue tests were conducted on specimens with saw-cut lengths of  $3/8$  in.,  $3/4$  in. and 2 in. As seen in the following tabulation, increasing the initial crack length resulted in an increase in the initial rate of crack growth.

<u>Initial-Notch Length (<math>2 l_0</math>) in.</u>	<u>Initial Rate of Crack Growth in./cycle x <math>10^6</math></u>
3/8	85
3/4	160
2	250

The maximum tensile strain at the tip of the notch was measured during the first cycle of load for specimens with 2-in. and 3/8-in. saw cuts to investigate the effect of initial crack length on the maximum strain. The net section stress in both specimens was  $\pm$  33 ksi. The maximum tensile strain at the notch root in the specimen with a 2-in. saw cut was about  $3 \times 10^{-6}$  in./in. and in the specimen with a 3/8-in. saw cut was about  $2 \times 10^{-6}$  in./in. Therefore, the specimen with the longer saw cut had a greater strain at the tip of the notch than the specimen with the shorter notch thus accounting for the variation in initial rate of crack growth noted above.

Photoelastic Evaluation of Strain Distribution: The results of the photoelastic studies indicated the same general behavior as the results of the strain gage studies, i.e., the strain field ahead of the crack enlarged with increasing crack length until the rate of crack growth became linear. The strain field then remained fairly constant in extent and magnitude until the final stage of crack growth. A sequence of contours of maximum principal strain difference ( $\epsilon_1 - \epsilon_2$ ) for various numbers of cycles of loading during the test of Specimen RC-16 show this quite clearly (Figs. 15 and 16). Note that up to  $N = 14,860$  both the magnitude and extent of the highly strained region in the vicinity of the crack tip enlarged with increasing crack length even though the stress was kept constant. At approximately  $N = 15,000$  the rate of crack growth became linear as may be seen in Fig. 8. The strain distribution remained fairly constant during the linear stage of crack propagation and then began to decrease as the crack neared the edge of the specimen. A typical photograph from which the maximum principal strain difference contours were obtained is presented in Fig. 17.

Varying Stress Levels: A limited investigation was made of the effect of

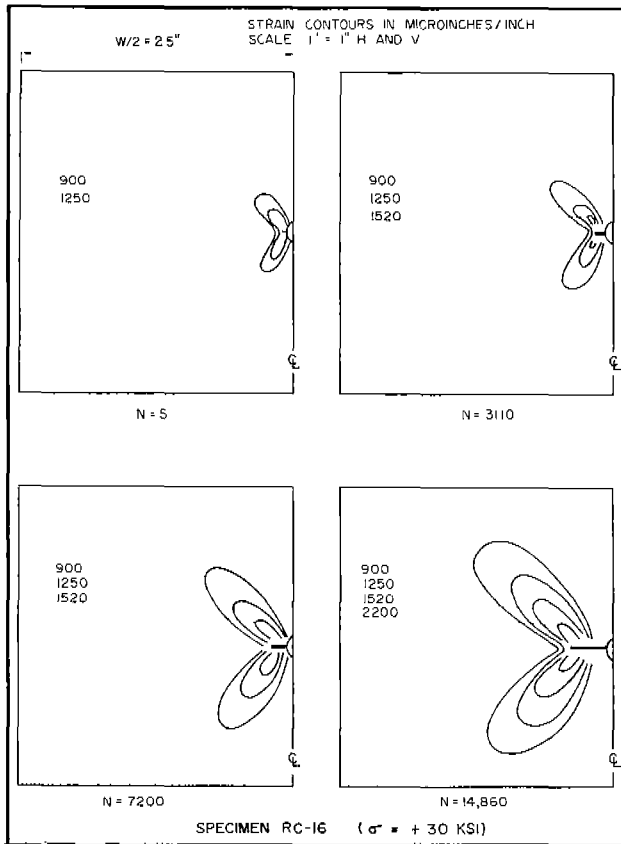


FIG. 15. CONTOURS OF MAXIMUM PRINCIPAL STRAIN DIFFERENCE ( $\epsilon_1 - \epsilon_2$ ) FOR VARIOUS CRACK LENGTHS

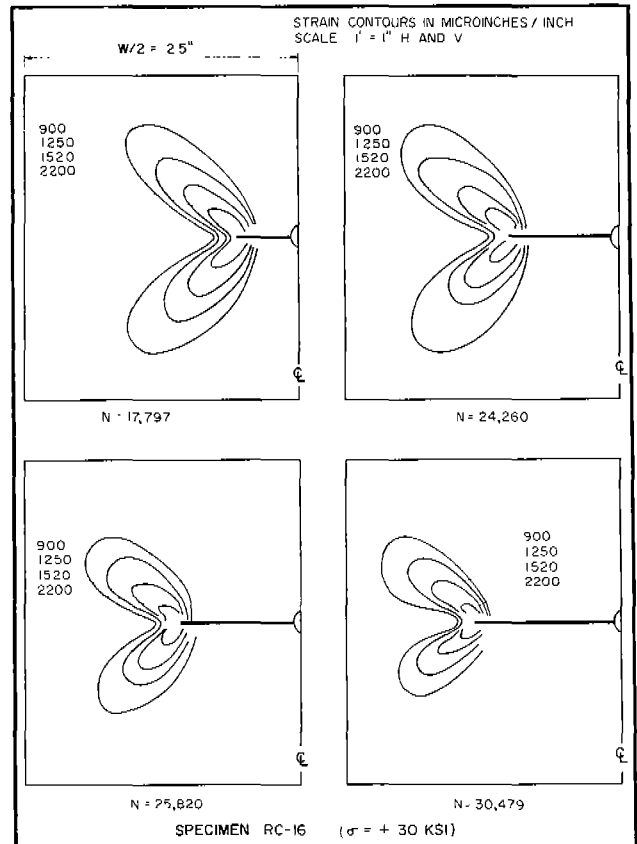


FIG. 16. CONTOURS OF MAXIMUM PRINCIPAL STRAIN DIFFERENCE ( $\epsilon_1 - \epsilon_2$ ) FOR VARIOUS CRACK LENGTHS

prior loading on the linear rate of crack growth. After establishing the linear rate of growth in a constant-stress test, the stress level was changed from  $\pm 27$  ksi to  $\pm 30$  ksi in one case (Specimen RC-18) and from  $\pm 30$  ksi to  $\pm 27$  ksi in the other case (Specimen RC-19) as may be seen in Fig. 18. The linear rates of growth for these tests were as follows:

Specimen Number	Stress Level ksi	Linear Crack Growth Rate in./cycle x $10^6$	Second Stress Level ksi	Linear Crack Growth Rate in./cycle x $10^6$
RC-18	$\pm 27$	25	$\pm 30$	60
RC-19	$\pm 30$	54	$\pm 27$	30

On the basis of these limited results, it would appear that, in the linear stage

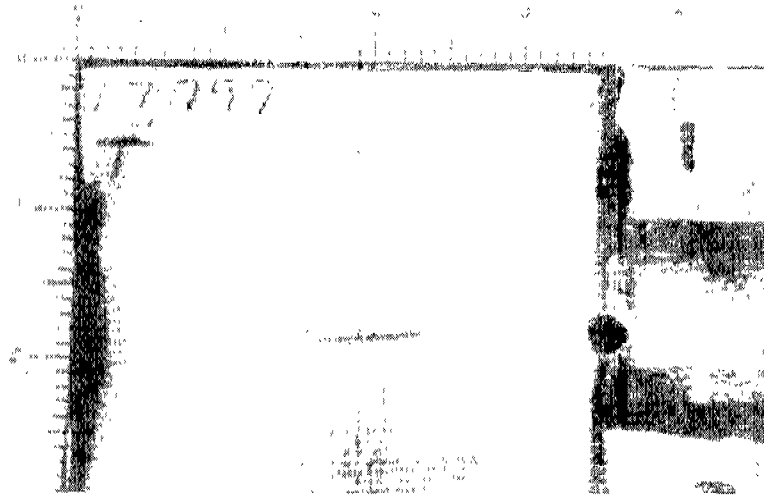


FIG. 17. TYPICAL PHOTOGRAPH OF MAXIMUM PRINCIPAL STRAIN CONTOURS

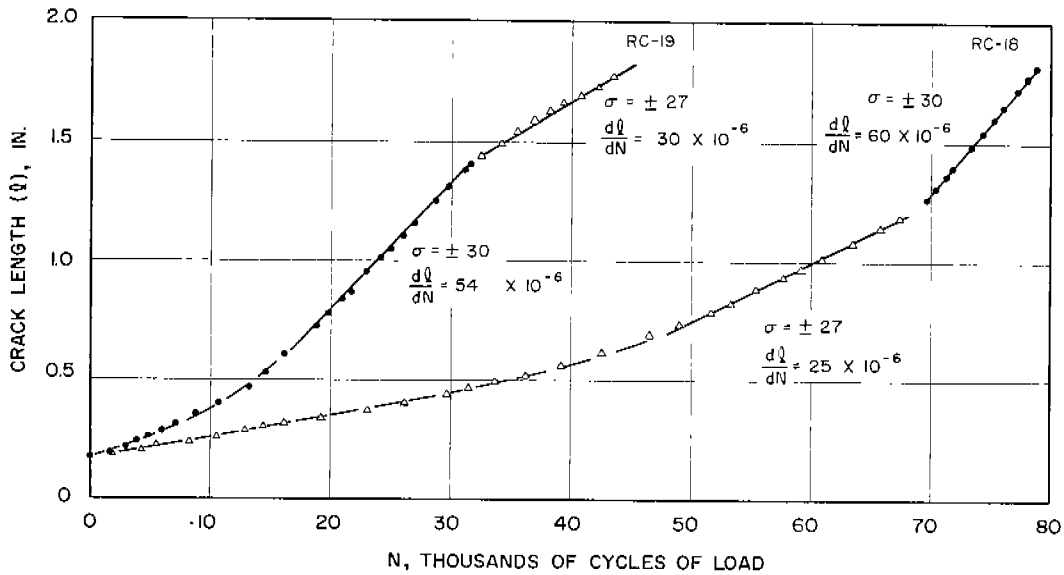


FIG. 18. CRACK PROPAGATION FOR MULTIPLE STRESS LEVELS

and at high-stress levels, prior loading history has little effect on the subsequent rate of fatigue crack propagation. This would suggest that crack propagation is a factor which can be summed for different stress levels and thus in some instances may be a valuable means of studying fatigue damage.

Studies by Hudson and Hardrath<sup>35</sup> indicate that prior loading history does have an effect on rate of crack growth if the difference in stress levels

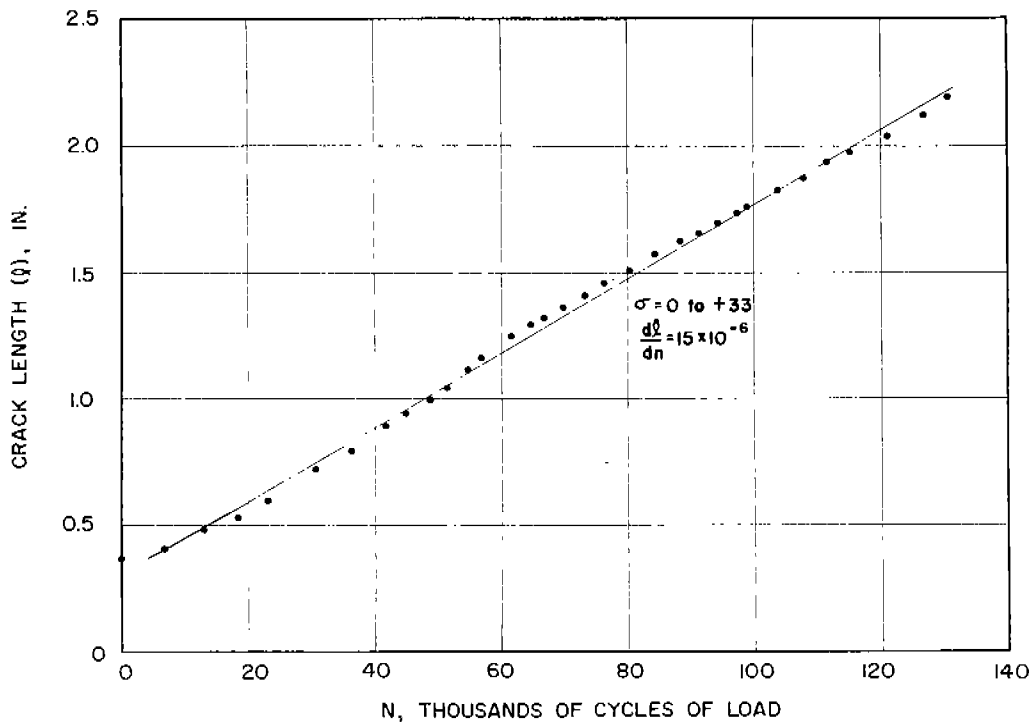


FIG. 19. CRACK PROPAGATION IN 0-TO-TENSION CONSTANT-STRESS TEST

is large. However, they observed that as the stress levels are increased and as the difference between the stress levels is made smaller the effect of prior loadings is reduced. The results of their constant-load tests, at the smaller differences in stress levels, are in agreement with the general results found for the two constant-stress tests described above.

Zero-to-Tension Constant-Stress Test: One specimen was tested at  $\sigma = + 33$  ksi to evaluate the fatigue behavior of a plate specimen under conditions of 0-to-tension loading. As expected, a linear relationship existed between  $l$  and  $N$  for the major portion of the test (see Fig. 19). An indication of the importance of total range of loading and compressive loading rather than just the maximum load can be obtained by comparing the crack-growth data from the various tests. The linear rate of crack propagation for the 0 to + 33 ksi stress cycle was  $15 \text{ in./cycle} \times 10^6$  whereas the linear rate of crack propagation for the  $\pm 33$  ksi stress cycle was  $230 \text{ in./cycle} \times 10^6$ .

Zero-to-tension constant-stress tests conducted by Weibull<sup>23, 29</sup> on aluminum sheets showed the same general behavior for the major portion of the life of his specimens.

Effect of Temperature and Aging

Temperature: In general, lowering the temperature of steels increases their strength but decreases their ductility. For unnotched specimens, the yield strength, ultimate strength and fatigue limit increase with decreasing temperature.<sup>36-38</sup> Since the fatigue limit increases at lower temperatures, it would be reasonable to expect the rate of fatigue crack propagation to decrease.

Tensile tests on the material used in this investigation showed that for unaged specimens, the upper yield point was increased from 41.6 ksi to 46.1 ksi by lowering the test temperature from 78 F to -40 F. For these two temperatures there was no significant change in ductility. The tensile properties of this material at -40 F are presented in Table 1.

Four constant-stress fatigue tests were conducted at -40 F to study the effect of temperature on rate of crack growth. The test stress was  $\pm 30$  ksi for all specimens; two specimens were aged and two were unaged. The temperature of -40 F was chosen because it was a convenient test temperature well below the 15 ft-lb Charpy V-notch impact value (Fig. 2).

In comparison to the rates at 78 F the rate of crack growth in all four tests decreased markedly. However, there was negligible variation in the behavior of specimens tested at -40 F indicating that the rate of fatigue-crack growth may be insensitive to aging at low temperatures. The crack growth rates for specimens tested at -40 and 78 F are presented in the following tabulation. All specimens were tested at  $\sigma = \pm 30$  ksi.

AGED			UNAGED		
Specimen Number	Temperature °F	Linear Crack Growth Rate in./cycle x 10 <sup>6</sup>	Specimen Number	Temperature °F	Linear Crack Growth Rate in./cycle x 10 <sup>6</sup>
7-in.-Wide Specimens					
RC-26	-40	25	RC-20	-40	25
RC-19	78	54	RC-16	78	95
5-in.-Wide Specimens					
RC-28	-40	20	RC-27	-40	21
RC-34	78	50	RC-31	78	77

In addition to the decrease in growth rates, the time required to initiate the crack and the initial stage of fatigue crack growth were increased. Therefore the total fatigue lives at -40 F would be much longer than at 78 F. The crack growth curves for these four tests are presented in Fig. 10.

Aging: Strain aging of mild steel is the change which takes place as a result of cold working followed by an "aging" or precipitation process in which carbon and nitrogen atoms are presumed to strengthen the metal by diffusing to dislocations in the crystal lattice. The aging process occurs at room temperatures over a long period of time but is markedly accelerated at temperatures only slightly above ambient. This combination in susceptible steels of prior cold work and aging results in increased yield strength and hardness, and decreased ductility. In addition, aging may make some steels more susceptible to brittle fracture.<sup>39-40</sup> Rally and Sinclair<sup>41</sup> found that the shape of an S-N curve may be influenced by strain aging. In addition, they noted that, "strain aging appears to influence the rate of crack propagation, however, quantitative predictions on the location of the knee cannot be made since the relationship between temperature and rate of crack propagation is not known."

In the investigation reported herein, no attempt was made to evaluate the effect of various strain aging or aging conditions but merely to use one aging condition. Based on studies of a similar mild steel by other investigators,<sup>42</sup> the specimens were aged at 150 C (302 F) for 90 minutes.

The specimens were not strained prior to aging so that the effect of aging alone on the rate of crack growth at different temperatures could be studied.

Since the specimens were not strain aged, but merely aged, a significant change in material properties would not be expected. This was indeed the case as the upper yield point increased only from 41.6 ksi to 43.3 ksi as a result of the aging and there was no significant change observed in the ductility. A detailed comparison of the tensile properties of aged and unaged specimens is presented in Table 1.

In the fatigue tests of specimens at 78 F the linear rate of crack growth was lower for aged specimens than it was for unaged specimens in all cases except one. The one exception was at the highest stress level at which both

aged and unaged specimens were tested,  $\sigma = \pm 33$  ksi. In this instance the linear rates were almost the same, i.e.,  $237 \times 10^{-6}$  in./cycle for the aged specimen and  $230 \times 10^{-6}$  in./cycle for the unaged specimen. For specimens tested at lower stress levels the difference in linear rate of crack growth between aged and unaged specimens increased as shown in the following tabulation:

Stress Level ksi	Specimen Width in.	Linear Rate of Crack Growth, in./cycle $\times 10^6$	
		Aged Specimens (Specimen Nos. in Parentheses)	Unaged Specimens (Specimen Nos. in Parentheses)
$\pm 33$	5	237 (RC-35)	230 (RC-33)
$\pm 30$	7	54 (RC-19)	95 (RC-16)
	5	50 (RC-34)	77 (RC-31)
$\pm 27$	7	25 (RC-18)	40 (RC-21)
	5	16 (RC-29)	29 (RC-30)

However, as may be seen in the crack growth curves of Figs. 9 and 10, the fatigue life of an aged specimen tested at room temperature was always greater than that of a comparable unaged specimen because of a longer initial crack propagation stage and, in all cases except one, a lower crack growth rate.

There was no difference in the linear rates of crack propagation between the aged and unaged specimens tested at -40 F (see Table 2 and Fig. 11). Thus, at low temperatures there apparently is no significant effect of aging on the rate of crack growth or the life.

## SUMMARY AND CONCLUSIONS

### Summary

This investigation has been conducted to study the parameters affecting crack propagation in low-cycle fatigue of mild steel. Flat plate specimens, centrally notched to reduce the number of cycles required to initiate the fatigue cracks, were subjected to reversal of axial loading. Three types of repeated load cycles were studied: constant load, reduced load, and constant stress.



The constant-stress tests were conducted at stress levels ranging from  $\pm 27$  ksi to  $\pm 36$  ksi, on specimens with widths of 5 in. and 7 in., at test temperatures of 78 F and -40 F and for both unaged and aged specimens.

A hypothesis relating the rate of crack growth and the stress has been presented to describe the behavior during various stages of propagation. In addition, the test results obtained in this study have been correlated with existing theories of crack propagation.

### Conclusions

On the basis of the study reported herein it may be concluded that:

(1) The De Forest theory that fatigue life of a member may be most realistically divided into an initiation stage and a propagation stage has been confirmed by the different tests conducted in this study; fatigue crack initiation is primarily influenced by the conditions near the point of origin while fatigue crack propagation is affected more by the conditions throughout the entire cross-section that the crack traverses.

(2) During the propagation stage the type of loading cycle will affect the fatigue behavior markedly.

- (a) In constant-load tests, in which the stress increases throughout the test, the rate of crack growth continuously increases.
- (b) If the maximum stress range is reduced throughout the test, as in a reduced-load test, the rate of crack growth will decrease throughout the test.
- (c) In a constant-stress test, in which the stress range is maintained constant during the test, the rate of fatigue crack propagation remains constant after a short initial period.

In most structures, depending upon their size, fatigue cracks will generally grow for some distance without changing greatly the over-all stress distribution. Thus it is believed that constant-stress tests more closely approximate the fatigue crack propagation behavior of actual structures than do the other types of tests.

(3) The fatigue crack propagation behavior during a constant-stress

test may be divided into an initial, linear, and final stage. The initial stage is a relatively short period in the total life of a specimen and is affected by the stress level, the number of cycles to crack initiation, initial geometry and changing stress field around the crack tip. During this period the rate of crack growth is proportional to the crack length and may be expressed as:

$$\frac{d\ell}{dN} = k\ell$$

In this initial stage, there is little difference in the behavior of specimens subjected to constant-load or constant-stress conditions.

After the initial stage, a linear rate of crack growth occurs and may be expressed as:

$$\frac{d\ell}{dN} = K \sigma^a$$

This linear rate of growth was observed in all constant-stress tests regardless of stress level, test temperature, initial geometry and for both unaged or aged specimens.

The third or final stage of propagation occurs as a crack nears the edges of a specimen. In this stage the behavior is affected by eccentricity in the specimens and edge effects.

(4) In the initial stage of crack propagation during which the rate of crack growth increases with crack length, the strain field ahead of the crack tip also increases in extent and magnitude. However, during the linear stage or major portion of the life of a member subjected to a constant-stress condition, both the rate of crack growth and the strain field ahead of the crack remain essentially constant. It is expected that this "steady-state" condition would exist for a considerable distance of crack propagation if the specimen were wide enough to be considered semi-infinite.

(5) Using the fact that the rate of crack propagation is primarily a function of the stress ( $d\ell/dN = K \sigma^a$ ), one can determine the number of cycles of loading required to propagate a crack through any distance L, for a condition of constant stress, by using the relationship:

$$N_L = \frac{L}{d\ell/dN}$$

(6) A linear rate of crack growth was found to occur in a 0-to-tension constant-stress test as well as in the complete reversal tests.

(7) A limited study of the effect of multiple loading levels indicated that at high-stress levels, prior loading history has little effect on the subsequent rate of fatigue crack propagation. This would suggest that crack propagation is a factor which can be summed for different stress levels and thus in some instances may be a valuable means of studying fatigue damage.

(8) Lowering the testing temperature from 78 F to -40 F reduced the rate of crack growth markedly and increased the fatigue life.

(9) Aging without prior straining had only a minor beneficial effect on the fatigue life of the steel tested.

#### REFERENCES

1. Bennett, J. A., "The Distinction between Initiation and Propagation of a Fatigue Crack," International Conference on Fatigue of Metals; London: The Institution of Mechanical Engineers, September 1956.
2. Thompson, N., and Wadsworth, N. J., "Metal Fatigue," Advances in Physics, 7:25 (January 1958).
3. Averbach, B. L., Felbeck, D. K., Hahn, G. T., and Thomas, D. A., editors, Fracture. New York: Technology Press and John Wiley and Sons, Inc., 1959.
4. International Conference on Fatigue of Metals. London: The Institution of Mechanical Engineers, September 1956.
5. Sines, G., and Waisman, J. L., Metal Fatigue. New York: McGraw-Hill, 1959.
6. "Basic Mechanisms of Fatigue," ASTM STP No. 237, 1958.
7. Sinclair, G. M., and Feltner, C. E., "Fatigue Strength of Crystalline Solids," Properties of Crystalline Solids (ASTM STP No. 283) 1960.
8. Parker, E. R., and Fegredo, D. M., "Nucleation and Growth of Fatigue Cracks," International Stresses and Fatigue in Metals. Amsterdam: Elsevier Publishing Co., pp. 263-283, 1959.

9. Grosskreutz, J. C., and Rollins, F. R., "Research on the Mechanisms of Fatigue," WADC Technical Report (No. 59-192), September 1959.
10. Vedeler, G., A Naval Architect's Reflections on Some Research Problems with Ship Steel (Ship Structure Committee Report Serial No. SSC-140). Washington: National Academy of Sciences-National Research Council, August 4, 1961.
11. DeForest, A. V., "The Rate of Growth of Fatigue Cracks," Journal of Applied Mechanics, vol. 58, pp. A23-A25 (1936).
12. Wilson, W. M., and Burke, J. L., "Rate of Propagation of Fatigue Cracks in 12- by 3/4-in. Steel Plates with Severe Geometrical Stress-Raisers," The Welding Journal, 27:8, Research Supplement, pp. 405-s-408-s (August 1948).
13. Head, A. K., "The Growth of Fatigue Cracks," Philosophical Magazine, 44:356 (7th series), pp. 925-938 (September 1953).
14. Head, A. K., "The Propagation of Fatigue Cracks," Journal of Applied Mechanics, vol. 23, p. 407 (1956).
15. McClintock, F. A., "The Growth of Fatigue Cracks under Plastic Torsion," International Conference on Fatigue of Metals. London: The Institution of Mechanical Engineers, September 1956.
16. Hult, J. A. H., "Fatigue Crack Propagation in Torsion," Journal of Mechanics and Physics of Solids, 6:1, pp. 47-52 (1957).
17. Martin, D. E., and Sinclair, G. M., "Crack Propagation under Repeated Loading," Proc., Third U. S. National Congress of Applied Mechanics, pp. 595-604, 1958.
18. Liu, H. W., "Crack Propagation in Thin Metal Sheet under Repeated Loading," Trans. ASME, 83:1, Series D (March 1961).
19. Frost, N. E., and Dugdale, D. S., "Fatigue Tests on Notched Mild Steel Plates with Measurements of Fatigue Cracks," Journal of the Mechanics and Physics of Solids, vol. 5, pp. 182-192 (1957).
20. Frost, N. E., and Dugdale, D. S., "The Propagation of Fatigue Cracks in Sheet Specimens," Journal of the Mechanics and Physics of Solids, vol. 6, pp. 92-110 (1958).
21. McEvily, A. J., Jr., and Illg, W., "The Rate of Fatigue--Crack Propagation in Two Aluminum Alloys," NACA TN 4394, 1958.

22. Illg, W., and McEvily, A. J., Jr., "The Rate of Fatigue--Crack Propagation for Two Aluminum Alloys under Completely Reversed Loading," NASA TN D-52, 1959.
23. McEvily, A. J., Jr., and Illg, W., "A Method for Predicting the Rate of Fatigue Crack Propagation," Proc. Symposium on Fatigue of Aircraft Structures, (ASTM STP No. 274), 1959.
24. Neuber, Heinz, Theory of Notch Stresses: Principles for Exact Stress Calculation. Ann Arbor, Michigan: J. W. Edwards, 1946.
25. Howland, R. C. J., "On the Stresses in the Neighborhood of a Circular Hole in a Strip under Tension," Trans. Philosophical Royal Society (London), 225:671, (Series A), pp. 49-86 (January 1930).
26. Weibull, W., "Basic Aspects of Fatigue," Colloquium on Fatigue, Stockholm (1955), Springer-Verlag, Berlin (1956): International Union of Theoretical and Applied Mechanics.
27. Weibull, W., "The Propagation of Fatigue Cracks in Light-Alloy Plates," NACA TN-25, SAAB Aircraft Co., 1954.
28. Weibull, W., "Effect of Crack Length and Stress Amplitude on Growth of Fatigue Cracks," The Aeronautical Research Institute of Sweden (Report 65), Stockholm, 1956.
29. Weibull, W., "Size Effects on Fatigue Crack Initiation and Propagation in Aluminum Sheet Specimens Subjected to Stresses of Nearly Constant Amplitude," ibid, Report 86.
30. Massonnet, Cuvelier, G., and Kayser, G., "Etude des lois de la propagation de la fissure de fatigue dans des éprouvettes d'acier doux soumises à flexion," Extrait du Bulletin du Centre d' Etudes de Recherches et d' Essais Scientifiques du Genie Civil, Tome XI, 1960.
31. Stallmeyer, J. E., Nordmark, G. E., Munse, W. H., and Newmark, N. M., "Fatigue Strength of Welds in Low-Alloy Structural Steels," The Welding Journal, 35:6, Research Supplement, pp. 298-s-307-s (June 1956).
32. McMaster, Robert C., ed., Nondestructive Testing Handbook (vol. II), Society for Nondestructive Testing, Ronald Press Co., 1959.
33. Tavernelli, J. F., and Coffin, L. F., Jr., "A Compilation and Interpretation of Cyclic Strain Fatigue Tests on Metals," Trans. ASM, vol. 51, p. 438 (1959).

34. Timoshenko, S., and Goodier, J. N., Theory of Elasticity. New York: McGraw Hill, p. 201, 1951.
35. Hudson, C. M., and Hardrath, H. F., "Effects of Changing Stress Amplitude on the Rate of Fatigue-Crack Propagation in Two Aluminum Alloys," NASA TN D-960, 1961.
36. Spretnak, J. W., Fontana, M. G., and Brooks, H. E., "Notched and Unnotched Tensile and Fatigue Properties of Ten Engineering Alloys at 25°C and -196°C," Trans. ASM, vol. 43, pp. 547-570 (1951).
37. Zambrow, J. L., and Fontana, M. G., "Mechanical Properties, Including Fatigue Properties at Very Low Temperatures," Trans. ASM, vol. 41, pp. 480-518 (1949).
38. Campbell, J. E., Review of Current Data on the Tensile Properties of Metals at Very Low Temperatures (DMIC Report 148). Columbus, Ohio: Battelle Memorial Institute, February 14, 1961.
39. Parker, E. R., Brittle Behavior of Engineering Structures. New York: John Wiley & Sons, Inc., 1957.
40. Dieter, G. E., Jr., Mechanical Metallurgy. New York: McGraw Hill, 1961.
41. Rally, F. C., and Sinclair, G. M., Influence of Strain Aging on the Shape of the S-N Diagram (Technical Report No. 45, Office of Naval Research Contract No. N60ri-071(04)). Urbana: University of Illinois, T and AM Department, June 1955.
42. Drucker, D. C., Mylonas, C., and Lianis, G., "Exhaustion of Ductility of E-Steel in Tension Following Compressive Prestrain," The Welding Journal, 39:3, Research Supplement, p. 117-s (March 1960).

#### ACKNOWLEDGMENT

The tests and analysis reported herein were conducted at the University of Illinois as a part of the Low-Cycle Fatigue program (SR-149) sponsored by the Ship Structure Committee through the Bureau of Ships, U. S. Navy, with the assistance of a Project Advisory Committee of the NAS-NRC. The investigation is a part of the structural research program of the Department of Civil Engineering of which Dr. N. M. Newmark is head. The authors wish to express their appreciation to a number of University staff members who assisted in the investigation in various ways and to the NAS-NRC staff members who assisted in the final editing of this report.

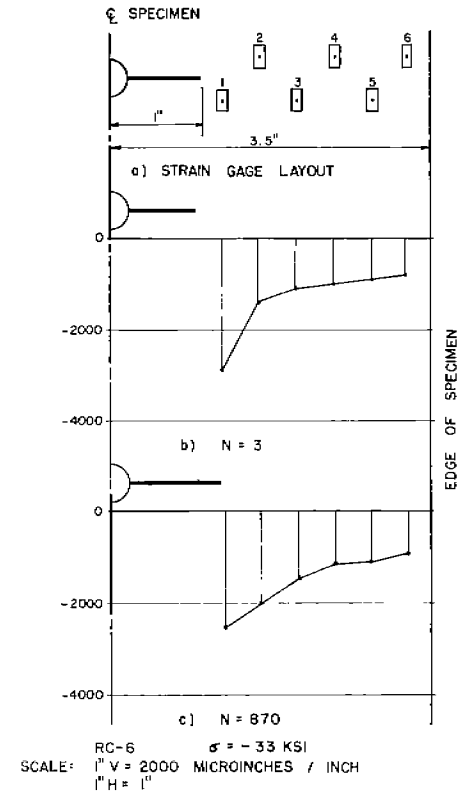
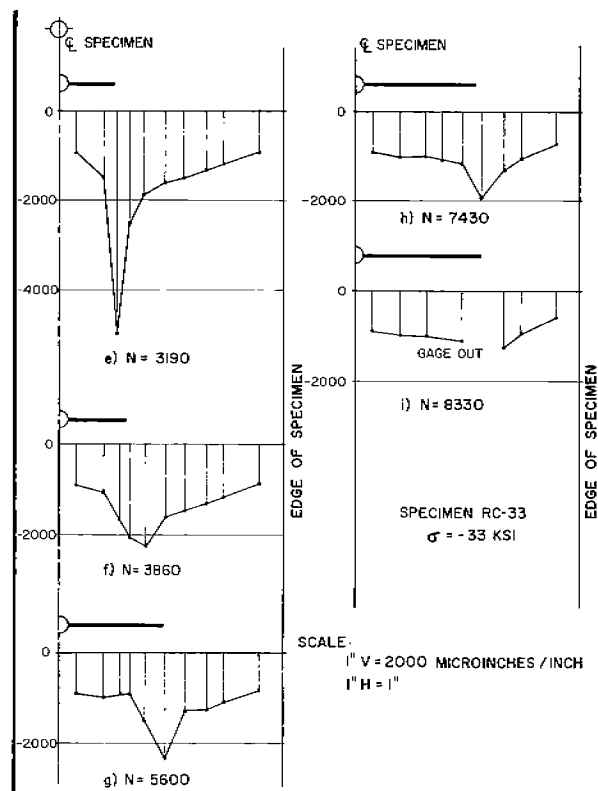
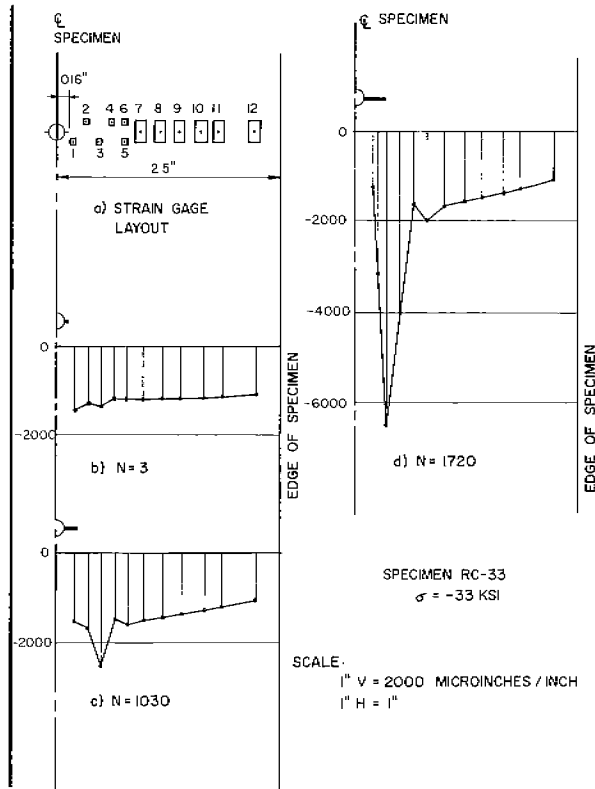
APPENDIX A

STUDY OF COMPRESSIVE LOAD CARRIED BY PARTIALLY CRACKED SPECIMEN

To investigate the compressive load carrying capacity of a cracked specimen, strain gages were placed slightly above or below the expected crack path on several specimens. As the crack propagated past a strain gage, strain measurements could still be obtained since the gages were intact.

At various crack lengths, the 0-to-compression increments of strain were examined and indicated that the cracked portion of the member continued to carry as much compressive load as the uncracked portion carried. Except for the region near the crack tip, where the strain is increased because of the stress concentration effect of the crack tip, the compressive strain increments were essentially the same for both the uncracked and cracked portions of a specimen, as may be seen in Figs. A-1 to A-5. Thus the assumption that the maximum nominal compressive stress may be based on the original net area is valid.

Further proof of the relative uniformity of compressive strain distribution, regardless of the fatigue crack length, was obtained with photo-elastic strain measurements. Contours of maximum principal strain difference under compressive loading ( $\epsilon_1 - \epsilon_2$ ) were obtained for various crack lengths and are presented in Fig. A-6. It can be seen clearly in these figures that even when the crack increases in length, the compressive strain distribution remains relatively constant.





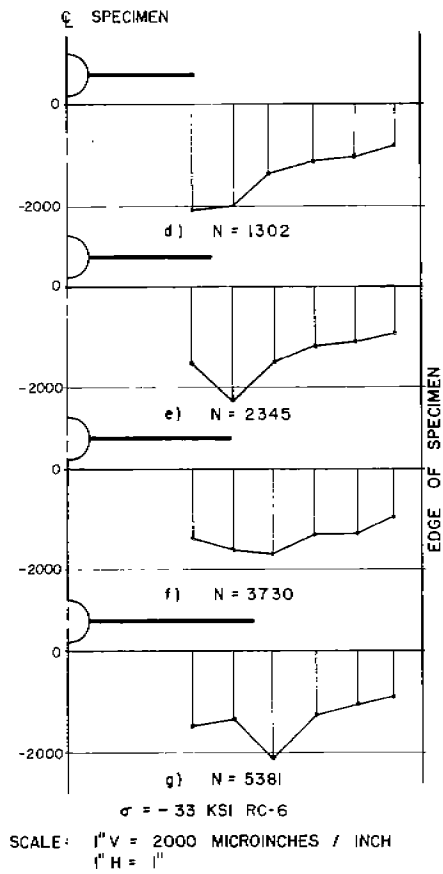


FIG. A-4. COMPRESSIVE STRAIN INCREMENTS FOR VARIOUS CRACK LENGTHS

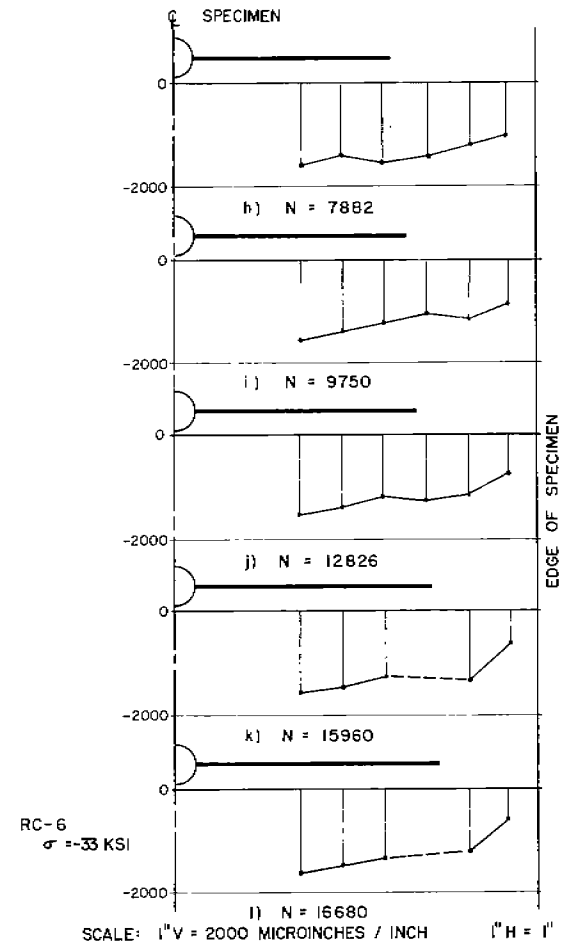


FIG. A-5. COMPRESSIVE STRAIN INCREMENTS FOR VARIOUS CRACK LENGTHS

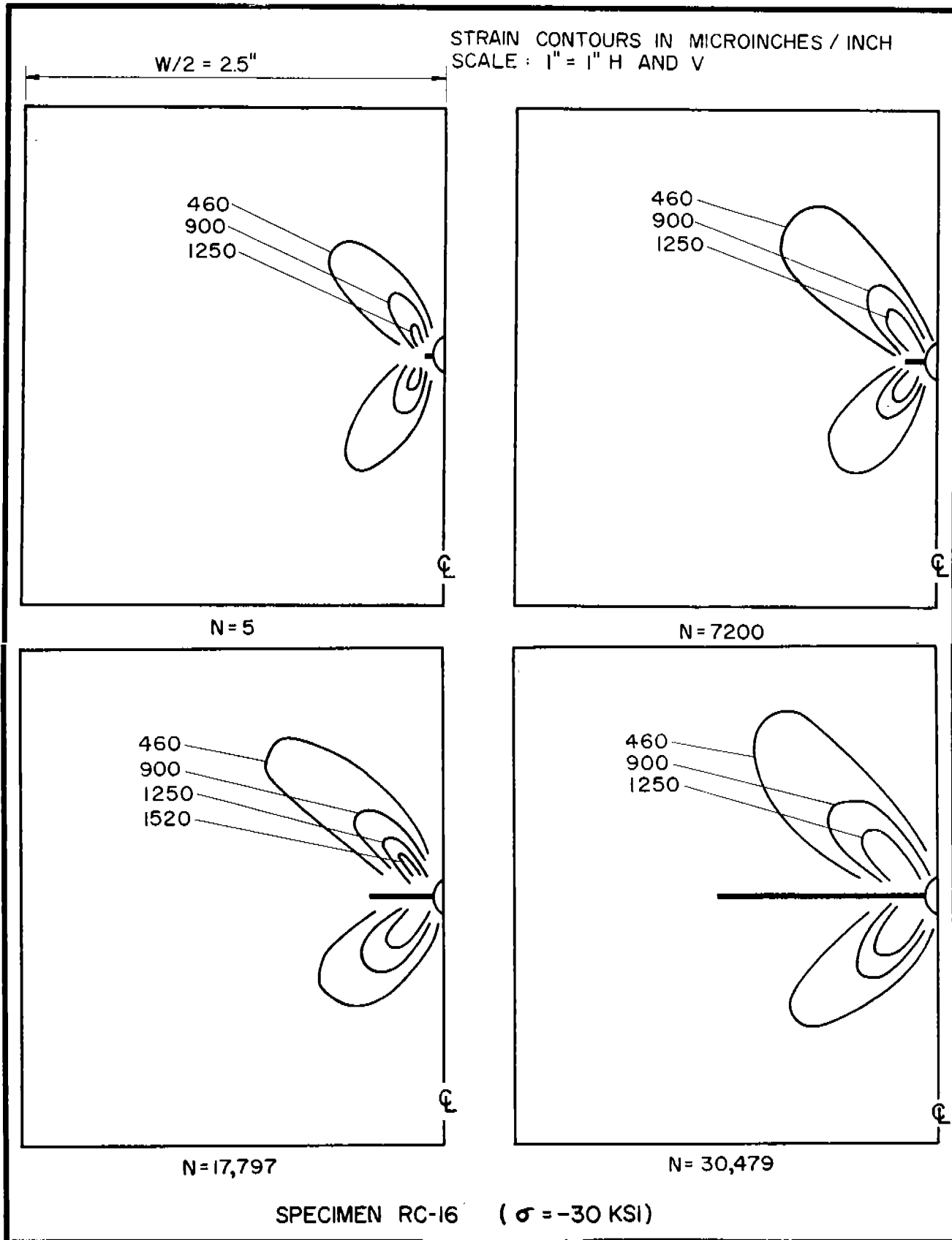


FIG. A-6. CONTOURS OF MAXIMUM PRINCIPAL STRAIN DIFFERENCE ( $\epsilon_1 - \epsilon_2$ ) FOR VARIOUS CRACK LENGTHS

APPENDIX B

CORRELATION OF EXISTING THEORIES WITH  
INITIAL STAGE OF CRACK PROPAGATION

Other investigators<sup>18-20</sup> have concluded that the rate of fatigue crack propagation in sheet specimen containing a small central slit should be proportional to the crack length and may be expressed as follows:

$$\frac{d\ell}{dN} = k\ell$$

$$\log \frac{\ell}{\ell_0} = k (N - N_0)$$

where

$\ell$  = half-length of crack (measured from the center-line of the specimen)

$N$  = number of cycles of loading

$k$  = coefficient of proportionality

$\ell_0$  = initial half crack length

$N_0$  = number of cycles of load corresponding to  $\ell_0$

Results of constant-load fatigue tests indicated that the above expression was valid only for crack lengths of less than about 1/8 the specimen width. Thus, measurements of crack growth vs. cycles of loading indicated a linear relationship when the crack length was plotted on a logarithmic scale. As the crack length became greater than about 1/8 the specimen width the rate of growth increased.

This same general behavior was observed in the constant-load tests conducted as a part of this investigation (see Fig. B-1). Note that initially there is a linear relationship between  $\log \ell$  and  $N$  ( $d\ell/dN = k\ell$ ) but, as the crack length increased the rate of crack propagation increased rapidly. Thus, the results of constant-load tests in which the stress range is continuously

increasing indicate that during the first part of the test the following relationship is valid.

$$\frac{d\ell}{dN} = k\ell$$

In a constant-stress test, the rate of crack growth remains linear after a short initial period. During the initial period, it was found that the relationship between  $\log \ell$  and  $N$  was the same as in the constant-load tests (see Fig. B-2). This behavior could be expected since for very short crack lengths there is little difference between a constant-load test and a constant-stress test. However, as the crack length increases, the linear relationship no longer exists between  $\log \ell$  and  $N$  as may be seen in Fig. B-2. The short lines perpendicular to the initial slopes of the crack growth curves mark the end of the initial stage of crack growth for each specimen. Thus, it can be seen that for the major portion of the life in a constant-stress test, there is a non-linear relationship between  $\log \ell$  and  $N$ .

In summary, it can be stated that for very short crack lengths the results of both constant-load tests and constant-stress tests agree with the results of other investigators.

$$\frac{d\ell}{dN} = k\ell$$

As the crack length increases however, this relationship is no longer valid for either constant-load tests or constant-stress tests.

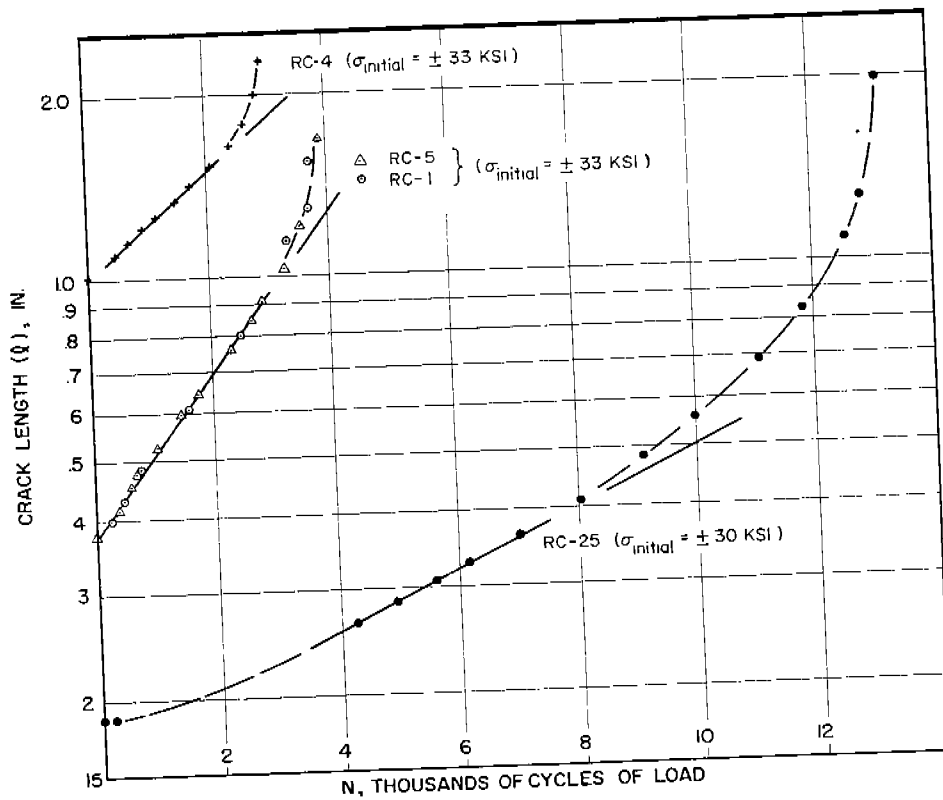


FIG. B-1. FATIGUE CRACK PROPAGATION FOR CONSTANT-LOAD TESTS

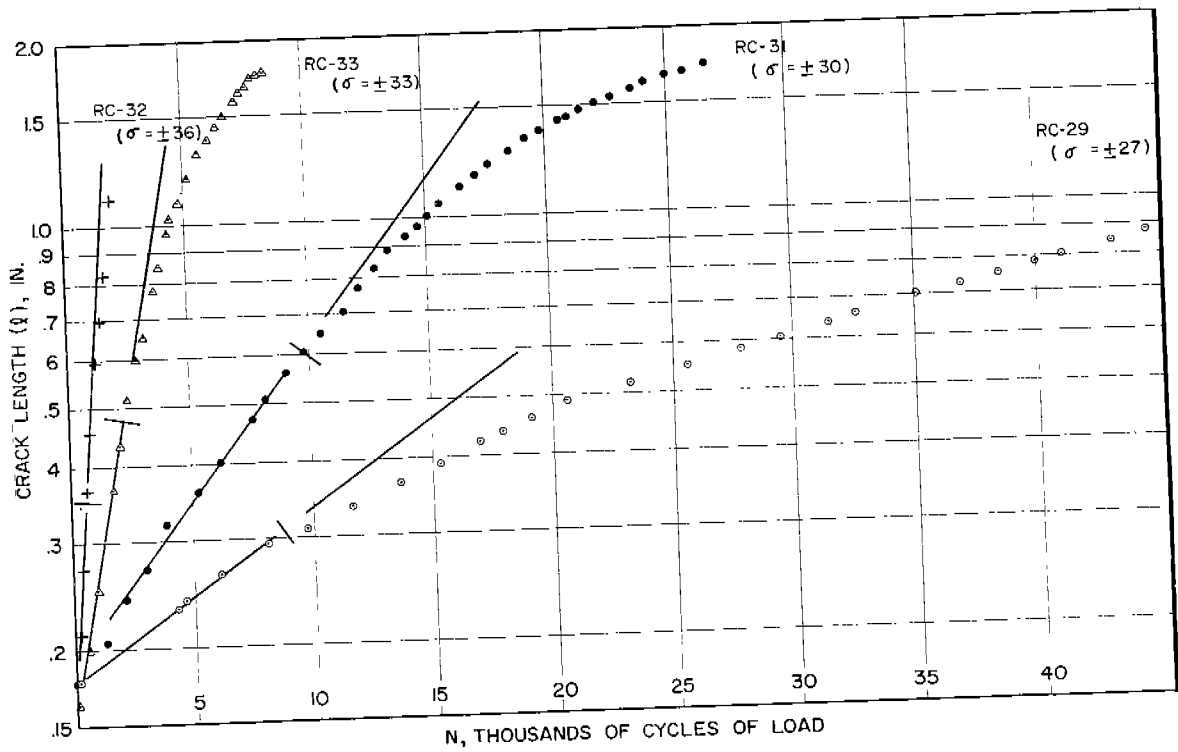


FIG. B-2. FATIGUE CRACK PROPAGATION FOR CONSTANT-STRESS TESTS

APPENDIX C  
STRAIN DISTRIBUTIONS

The 0-to-tension increments of strain for various crack lengths in four different specimens tested at four stress levels are presented in Figs. C-1 to C-5. A photograph showing a typical strain gage layout may be seen in Fig. 4. The following tabulation shows the specimen numbers and test stress levels. The general conclusions based on the results of these figures are discussed in the text.

<u>Figure Number</u>	<u>Specimen Number</u>	<u>Test Stress (<math>\sigma</math>), ksi</u>
C-1 and C-2	RC-30	$\pm 27$
C-3	RC-31	$\pm 30$
C-4	RC-35	$\pm 33$
C-5	RC-32	$\pm 36$

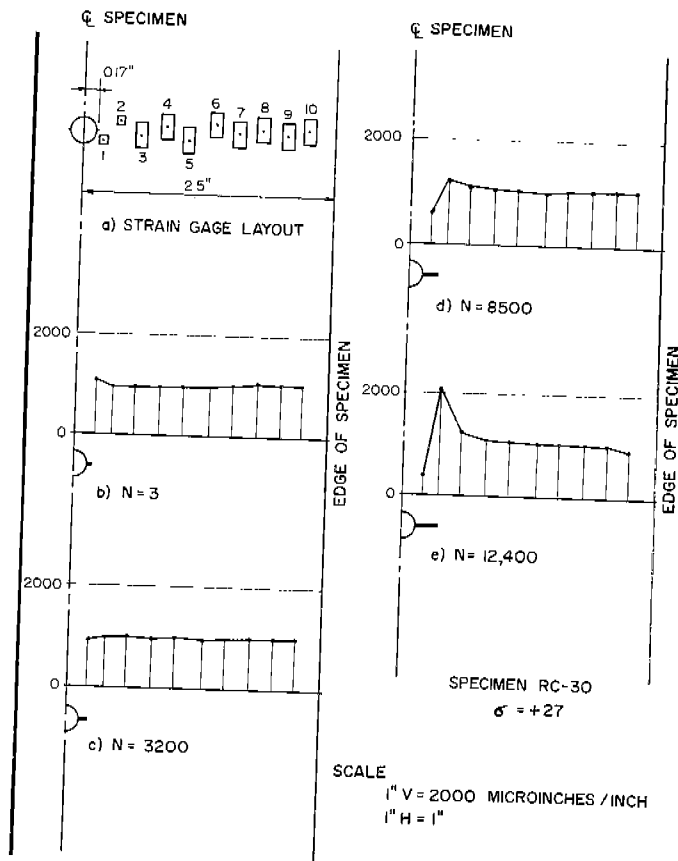


FIG. C-1. STRAIN GAGE LAYOUT AND TENSILE STRAIN INCREMENTS FOR VARIOUS CRACK LENGTHS

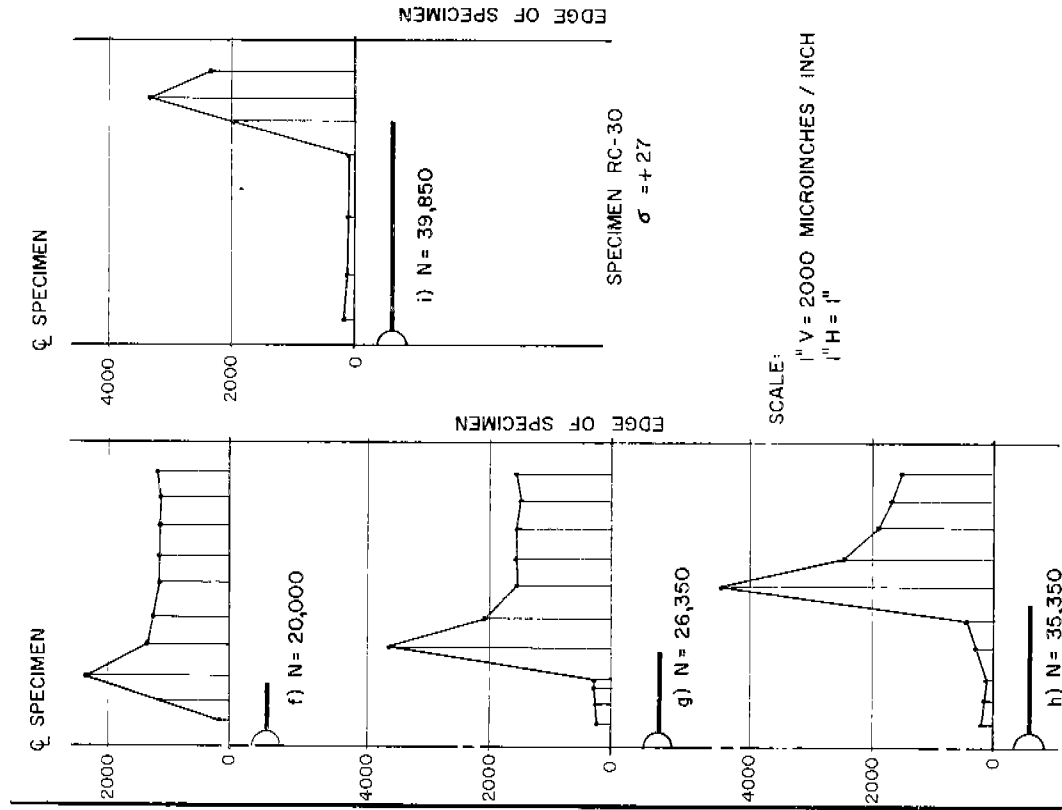
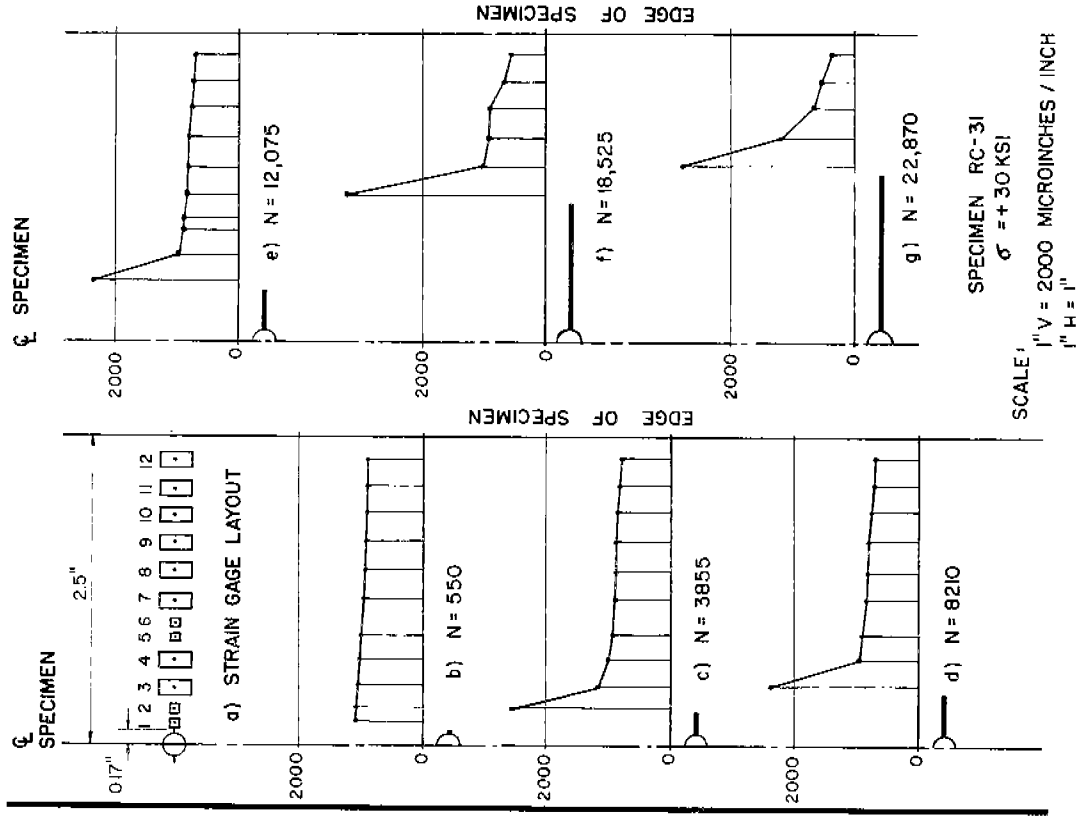


FIG. C-3. STRAIN GAGE LAYOUT AND TENSILE STRAIN INCREMENTS FOR VARIOUS CRACK LENGTHS

FIG. C-2. TENSILE STRAIN INCREMENTS FOR VARIOUS CRACK LENGTHS

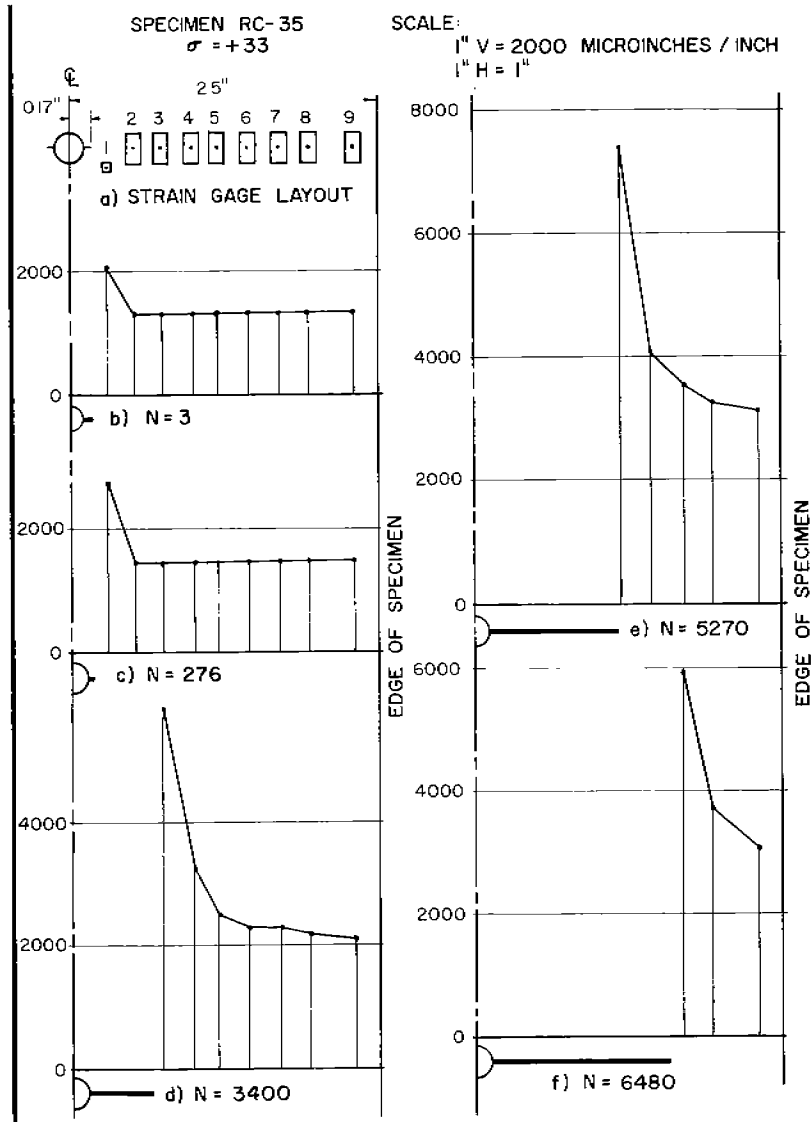


FIG. C-4. STRAIN GAGE LAYOUT AND TENSILE STRAIN INCREMENTS FOR VARIOUS CRACK LENGTHS

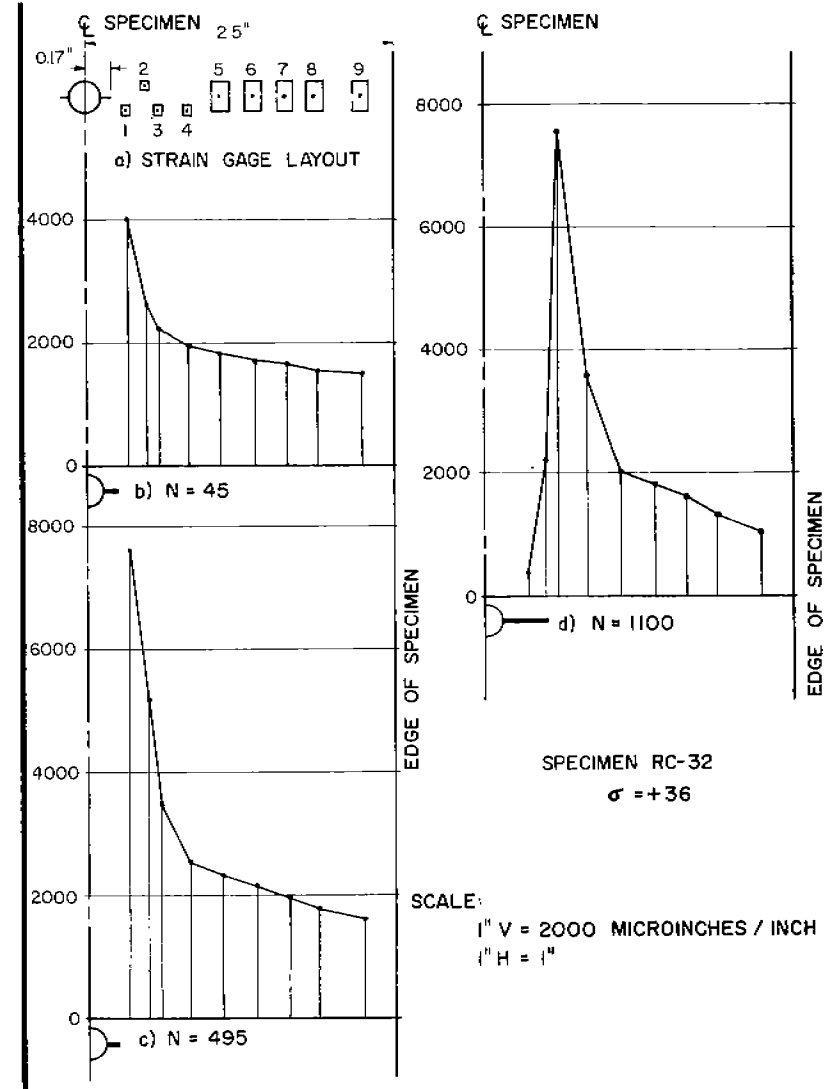


FIG. C-5. STRAIN GAGE LAYOUT AND TENSILE STRAIN INCREMENTS FOR VARIOUS CRACK LENGTHS



COMMITTEE ON SHIP STRUCTURAL DESIGN  
Division of Engineering & Industrial Research  
National Academy of Sciences-National Research Council

Chairman:

N. J. Hoff  
Head, Department of Aeronautics & Astronautics  
Stanford University

Vice Chairman:

M. G. Forrest  
Vice President, Naval Architecture  
Gibbs and Cox, Inc.

Members:

C. O. Dohrenwend  
Provost and Vice President  
Rensselaer Polytechnic Institute

J. H. Evans  
Department of Naval Architecture & Marine Engineering  
Massachusetts Institute of Technology

D. K. Felbeck  
Department of Mechanical Engineering  
University of Michigan

J. M. Frankland  
Mechanics Division  
National Bureau of Standards

William Prager  
Brown University

J. J. Stoker  
Director of Institute of Mathematical Sciences  
Department of Mathematics  
New York University

Dana Young  
Technical Vice President  
Southwest Research Institute

A. R. Lytle  
Director

R. W. Rumke  
Executive Secretary